NASA CONTRACTOR REPORT

NASA CR-7

NASA CR-728

STUDY OF A SIGNAL PROCESSOR EMPLOYING A SYNTHETIC PHASE ISOLATOR

by W. J. Bickford, R. G. Cease, D. B. Cooper, and H. J. Rowland

Prepared by
RAYTHEON COMPANY
Norwood, Mass.
for Electronics Research Center

NATIONAL AERONAUTICS AND SPACE ADMINISTRATION • WASHINGTON, D. C. • MAY 1967

NASA CR-728

STUDY OF A SIGNAL PROCESSOR EMPLOYING A SYNTHETIC PHASE ISOLATOR

By W. J. Bickford, R. G. Cease, D. B. Cooper, and H. J. Rowland

Prepared under Contract No. NAS 12-82 by
RAYTHEON COMPANY
Norwood, Mass.

for Electronics Research Center

NATIONAL AERONAUTICS AND SPACE ADMINISTRATION

For sale by the Clearinghouse for Federal Scientific and Technical Information
Springfield, Virginia 22151 – CFSTI price $3.00

T A B L E O F C O N T E N T S

TABLE OF SYMBOLS

A	generic term for input signal amplitude
A_i	input signal amplitude of the i^{th} channel
B	output amplitude
E_i	rms value of the i^{th} signal input
E_o	rms value of the output signal
F	transfer function of the IF filter
G	gain of the loop amplifier
H	transfer function of the AGC low pass filter
J_i	amplitude of the i^{th} input noise wavelet
N_o	power spectral density of the input noise
T_o	elapsed time
V_i	amplitude of the i^{th} IF
W	noise bandwidth of input
$z(t)$	input to AGC system
$b/2\pi$	bandwidth of the IF filters
c_i	perturbation in the i^{th} IF amplitude
α	input to the AGC system
δ	area under the noise pulse wavelets
ξ	phase of the δ-wavelet
η	step input to the AGC system
θ	phase of the signal output
λ	AGC gain
$\mu(t)$	perturbation on $z(t)$

TABLE OF SYMBOLS

(Continued)

ξ_i	phase of the i^{th} J-wavelet
ρ	phase of the η-step
σ	rms value of input noise = $\sqrt{N_0 W}$
τ	time constant of AGC
ϕ_i	phase of the i^{th} signal input
ψ_i	phase of the i^{th} IF perturbation
ω	generic symbol for radian frequency
ω_i	input signal frequency
ω_{if}	center frequency of IF filter
ω_o	output frequency

ABSTRACT

This report covers the analytical and experimental investigations pertaining to a signal data processor employing the Raytheon Synthetic Phase Isolator. The study shows analytical justification for considering such a signal processor in an adaptive antenna system. The experimental program demonstrated that the analytical conclusions were achievable, and all the desired results were demonstrated by a two-channel processor.

The Synthetic Phase Isolator, SPI, is a signal processing technique for combining signals which originated at one point but have travelled slightly different paths in reaching the receiver. If the radio frequency bandwidth is small compared to center frequency and the relative path delays are small compared to the time of one cycle of the highest information frequency, the SPI will perform its function which is that of a predetection combiner.

CONTRACT OBJECTIVE

The objective of this study is to conduct analytical and experimental investigations of a signal data processor employing a synthetic phase isolator. The study shall determine the feasibility and practicability of the isolator, to provide increased aperture gain by processing signal returns from multi-aperture antennas in one of two feedback configurations as specified by the cognizant NASA principal investigator.

INTRODUCTION

Techniques for predetection combining and adaptive antenna systems have been under investigation for many years. Early in 1965, Raytheon began investigation of a technique which acquired the name Synthetic Phase Isolator (SPI). This effort led to proving feasibility by some rather simple yet highly effective electronic breadboards. Further, preliminary performance analysis indicated that the technique could be incorporated in adaptive antenna systems and in multi-channel predetection combiner applications.

In October, 1965, NASA-ERL provided Raytheon further sponsorship to pursue this technique in the areas of more detailed analysis and the construction of a two-channel processor breadboard for signals centered at 70 mc and for multi-aperture applications. The program was focussed primarily at the regenerative version of the SPI without detracting from the effort required by the local-oscillator configuration. Figure 1 shows the signal processing technique as a receiving system of four antenna elements. The SPI processor as shown has as its basic element a regenerative loop. The loop produces oscillations at the processor IF filter frequency, in this case 28 mc. As there are four branches, each with a filter, the conditions for loop gain will depend in some manner upon the relative phase of the 28-mc signals. For now, it will be assumed that the circuits settle down in a manner that provides maximum loop gain, and that the AGC maintains the mean value of loop gain at unity. If this be true, then information common to all channels must add in phase at the summing circuit after being heterodyned

by the 28-mc signal. The consequence of this is that the relative phases of the 28-mc oscillations must be such as to cancel the relative phase differences of the information signals. In the main part of this report, the detail analysis establishes the loop stability and how, with linear elements, not only are the relative phase differences isolated but also the combined signal is the result of weighting the individual contributors to provide the maximum signal to noise.

The simplicity of this signal processor tends to mask the appreciation of its effectiveness. For information bearing signals, it is assumed that the signal, after combining, should have a favorable S/N ratio. This can be the result of many channels, each with very unfavorable S/N ratios.

The experimentation portion of the program was aimed at determining the feasibility of achieving the characteristics predicted by the analysis. Within the limitations of a two-channel processor, the theoretical results were demonstrated. The in-phase or coherent combining was demonstrated. This coherent combining was achieved for carrier-to-interference ratios from a favorable 20 db to an unfavorable -20 db without measurable change in performance. The ratio-squared combining feature also conformed to theory. The circuits used to demonstrate theory were designed at a 70-mc center frequency. The design bandwidth was 10 mc. The SPI technique proved effective in handling signals with a minimum of distortion. Two tone tests showed the third order products to be down about 50 db.

The body of this report is divided into two main sections. The first or analytical part is aimed at deriving the expected performance of the system. The second describes the techniques used to realize a practical processor. The results show that the favorable aspects of the analysis were achieved in a practical circuit configuration.

In addition to the work supported by this contract, Raytheon has conducted antenna pattern measurements using an early version of the SPI processor. This processor is a linear predetection combiner and uses an input frequency of 4.3 MHz. Copies of this report, "Adaptive Antenna Arrays, Predetection Element Combining using the Synthetic Phase Isolator" by H. J. Rowland, et al, accompany this report.

The authors wish to express their appreciation for the many helpful and probing discussions with Dr. L. C. Van Atta and Mr. George Haroules of NASA - ERC. They are particularly indebted to Dr. J. T. deBettencourt for his guidance and direction in relating this work to antenna systems and signal transmission characteristics.

OPTIMAL SPI RECEIVING SYSTEM

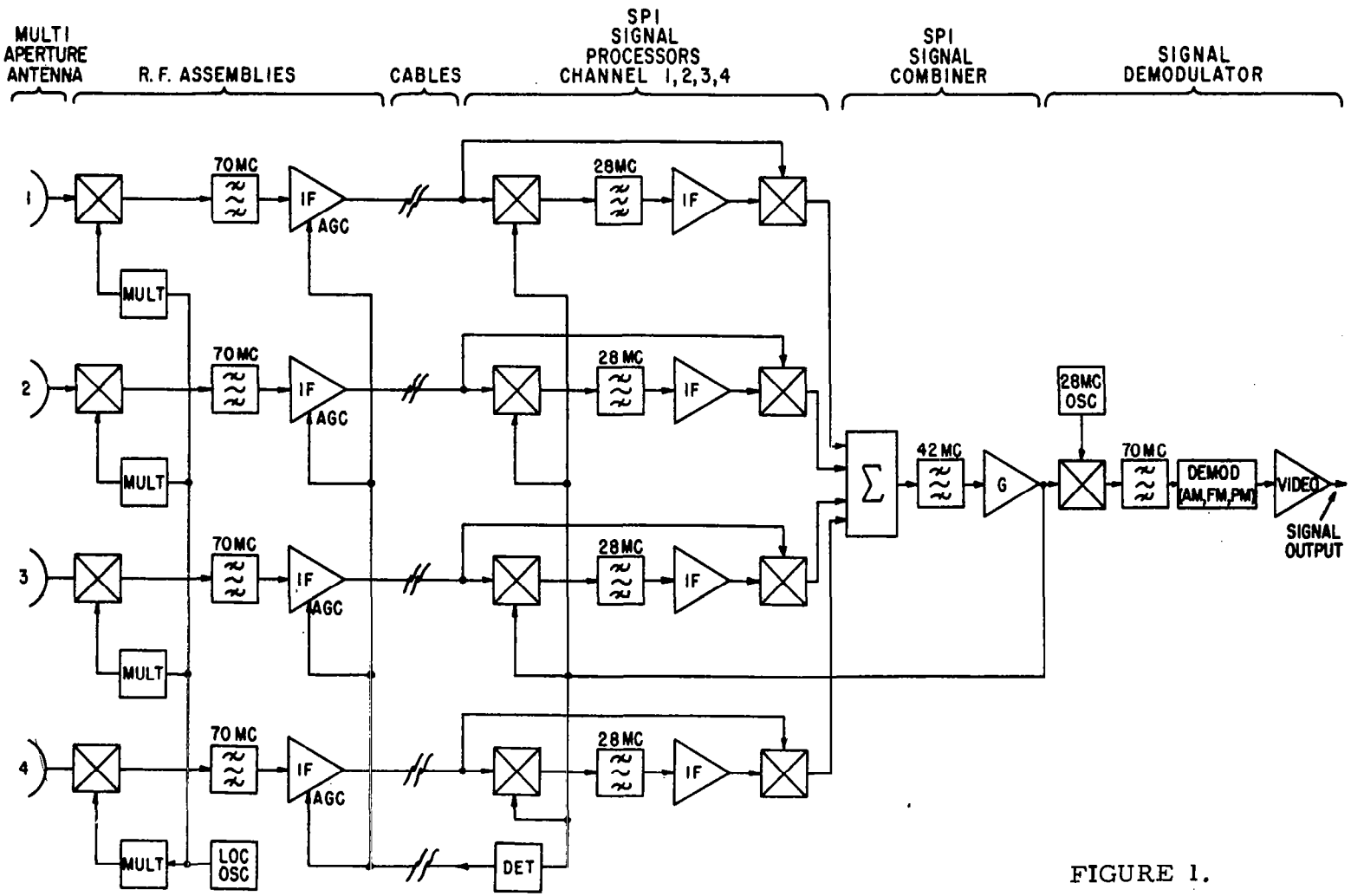

FIGURE 1.

RECOMMENDATIONS AND CONCLUSIONS

This study program has been particularly fruitful. The detailed analysis has borne out the preliminary predictions and extended these to show that a pre-detection combiner can be achieved that is essentially linear and does not appear to exhibit a threshold. The experimental program of a two input SPI has demonstrated the feasibility of realizing the desirable features of this technique with solid state components that exist today. The salient features demonstrated during the feasibility tests are:

1) The coherent pre-detection summation of information received via different paths or pre-detection combining,
2) ratio squared combining,
3) the lack of threshold.

Although the extent of the evaluation has been necessarily limited in this program the feasibility and practicality of the signal processing technique has been demonstrated. It follows that more complete testing would be desirable and in particular the number of channels involved in the tests should be significantly larger that two. The next set of tests should involve no less than four and preferably eight units.

As the intended application for this technique is with antenna arrays, work should be directed toward this area. First, the signal processor should be tested with simulated antenna signals. This involves signals undergoing varying transmission delays and varying transmission losses. Thus, a fading simulator should also be utilized.

When this technique is employed in physical systems and in particular space systems, the sky noise is involved. This interference may be considered as the specification of a noise source uniformly distributed over the sky pulse extended on large sources of radiation such as the sun plus many discrete sources. Analysis should be made of the behavior of the total system.

SIMPLIFIED THEORY OF OPERATION

The basic SPI configuration is shown in Figure 2. It is comprised of a correlator modulator, a narrow bandpass filter, a processor modulator, a low pass filter, and an AGC amplifier. It will be shown that the phase of the system output is independent of that of the system input.

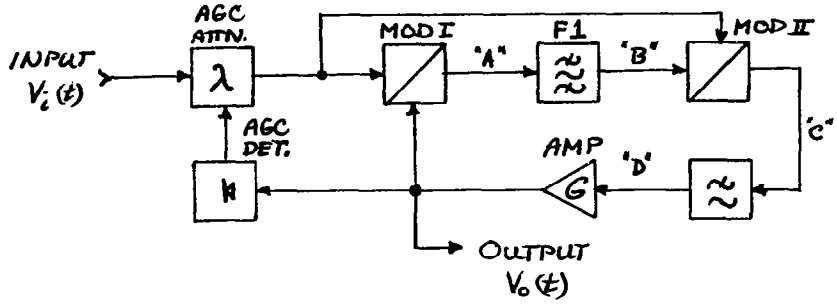

FIGURE 2

The two modulators are assumed to be ideal multipliers, F1 is assumed to be an infinitely narrow bandpass filter of center frequency ω_{if}, F2 is a low pass filter; the amplifier has a gain G, and the AGC has a gain λ. If the input $V_i(t) = A\cos(\omega_i t + \phi)$, and we assume an output of the form $B\cos(\omega_o t + \Theta)$, with B, ω_o, and Θ to be determined, at point A we have

$$\lambda AB\cos(\omega_i t+\phi)\cos(\omega_o t+\Theta) = \frac{\lambda AB}{2}\left[\cos\left[(\omega_i+\omega_o)t+\phi+\Theta\right]+\cos\left[(\omega_i-\omega_o)t+\phi-\Theta\right]\right]$$

An output can only exist at point B for $\omega_i+\omega_o=\omega_{if}$ or $\omega_i-\omega_o=\omega_{if}$. We will choose the lower sideband in filter F2, and thus $\omega_o=\omega_i-\omega_{if}$. Thus at point B we have $\frac{\lambda AB}{2}\cos(\omega_{if}t+\phi-\Theta)$, and this becomes, at point C, $\frac{\lambda^2 AB}{2}\cos(\omega_{if}t+\phi-\Theta)\cos(\omega_i t+\phi) = \frac{\lambda^2 A^2 B}{4}\left[\cos\left[(\omega_i+\omega_{if})t+2\phi+\Theta\right]+\cos\left[(\omega_i-\omega_{if})t+\Theta\right]\right]$.

We choose the lower sideband in filter F2, and at point D the signal is $\frac{\lambda^2 AB}{4}\cos[(\omega_1-\omega_{1,f})t+\Theta]$. Thus $V_o(t)=\frac{\lambda^2 ABG}{4}\cos[(\omega_1-\omega_{1,f})t+\Theta]=B\cos(\omega_o t+\Theta)$, and the value of AGC gain will adjust to maintain $|V_o|=B$, making $\lambda=\frac{2}{A\sqrt{G}}$.

The important result, however, is that there is no connection between the input and output phases. The system contains a regenerative loop which produces a signal having amplitude and frequency dependent on input amplitude and frequency, but whose phase is totally independent of input phase.

To make these results more general, let $A=A(t)$, $B=B(t)$, $\phi=\phi_0+\phi(t)$, $\Theta=\Theta_0+\Theta(t)$, and let the time constant of the AGC amplifier be long compared to the lowest frequency in $A(t)$. At point A we then have $\frac{\lambda}{2}A(t)B(t)\cos[\omega_{1,f}t+\phi_0+\phi(t)-\Theta_0-\Theta(t)]$. The narrow bandpass filter strips off all the sidebands on this signal, giving $\frac{\lambda}{2}\overline{AB}\cos(\omega_{1,f}t+\phi_0-\Theta_0)$. At point D we will then have $\frac{\lambda^2}{4}A(t)\overline{AB}\cos(\omega_1-\omega_{1,f})t+\phi(t)+\Theta_0)$ and $V_o(t)=\frac{\lambda^2}{4}A(t)[\overline{AB}G]\cos((\omega_1-\omega_{1,f})t+\phi(t)+\Theta_0)$ Thus $B(t)=\frac{\lambda^2}{4}[\overline{AB}G]A(t)$, $\Theta(t)=\phi(t)$. Further, $A(t)B(t)=\frac{\lambda^2}{4}A^2(t)[G\overline{AB}]$, thus $\overline{AB}=\frac{\lambda^2}{4}\overline{A^2}[G\overline{AB}]$, thus $\lambda=\frac{2}{A_{RMS}\sqrt{G}}$ as before.

Thus $B(t)$ is proportional to $A(t)$, $\Theta(t)$ is equal to $\phi(t)$, and the information on the input has been transferred to the output with the exception of the static component of the input phase, ϕ_0. It is important to note that no restriction has been put on the waveform ($A(t)$ and $\phi(t)$) other than it be possible to meet, in a practical sense, the stipulations mentioned for AGC response and filter bandwidth.

This signal processing technique can readily be used to construct a pre-detection. combiner. The feedback path is made common to all units, as shown in Figure 3.

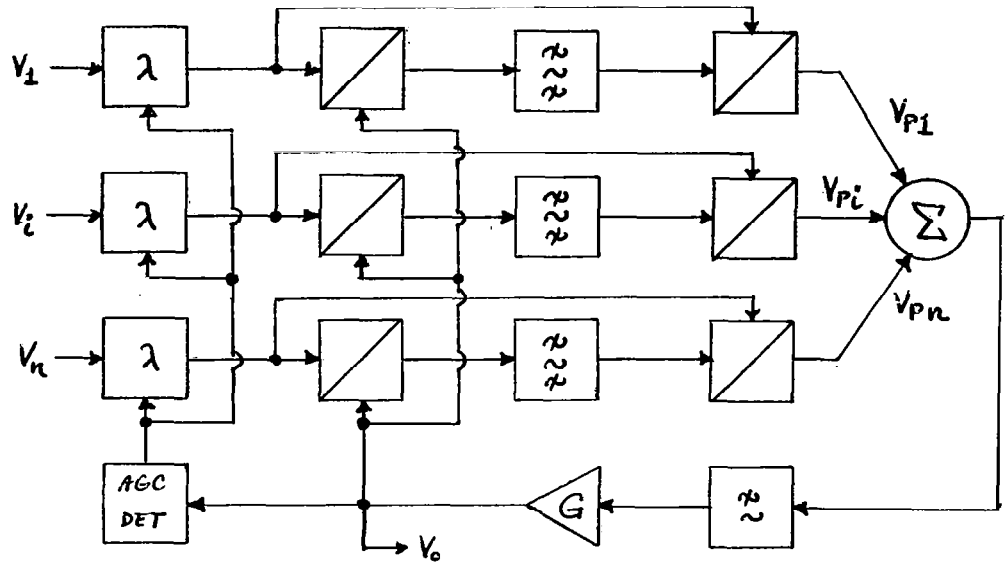

FIGURE 3

If the i^{th} input is denoted as $V_i = A_i \cos(\omega_1 t + \phi_i)$, and the output is assumed to be $B\cos[(\omega_1 - \omega_{IF})t + \theta]$, then by using the techniques in the previous section, it can be shown that $V_{Pi} = \frac{\lambda^2}{4} A_i^2 B \cos[(\omega_1 - \omega_{IF})t + \theta]$, and that the ϕ_i disappears. When the V_{Pi} add in the combiner, they all add in phase because their phases are all identical. The output is thus $V_o = \frac{\lambda^2}{4} BG[\Sigma A_i^2]\cos(\omega_o t + \theta)$ and $\lambda = \frac{2}{\sqrt{G\Sigma A_i^2}}$. The important point here is that the signals add up in voltage even though the ϕ_i are in general different.

It will now be shown that the SPI technique provides optimum (ratio squared) combining. For this computation we will assume that S/N at the output is much greater than one and the narrow-band filter F1 is infinitely narrow. These restrictions will later be re-examined. The rms noise inputs to the n channels are equal to σ and are uncorrelated, and the signal portion of the inputs, $E_i(t)$, is given by $A_i(t)\cos(\omega_1 t + \phi_i)$ with rms value E_i.

The output signal, E_o, will multiply with the input signal to produce a component at ω_{if}. Because filter F1 is infinitely narrow, no noise will appear on its output. Phase isolation will then take place, and the signals will add in phase. Because of the variation of the IF level in the various channels, the summation will be weighted by a factor K_i. The system output will then be given by

$$E_o = \sum_i K_i E_i$$

$$\sigma_o = \sqrt{\sum_i (K_i \sigma)^2} = \sigma \sqrt{\sum_i K_i^2}$$

then

$$\left(\frac{S}{N}\right)_o = \left(\frac{E_o}{\sigma_o}\right)^2 = \frac{\left[\sum_i K_i E_i\right]^2}{\sigma^2 \sum_i K_i^2}$$

Since the summation ΣK_i^2 can be held a relative constant, the output S/N will maximize when $\Sigma K_i E_i$ maximizes. This occurs when, in i-space, the vectors $\Sigma \vec{K_i}$ and $\Sigma \vec{E_i}$ are in the same direction. ($\vec{A} \cdot \vec{B}$ is a maximum when A and B are co-directional). If the vectors are co-directional, their components must be proportional, and $K_i = q E_i$

It then follows that

$$q = \sqrt{\frac{\sum K_i^2}{\sum E_i^2}}$$

Our weighting function K_i is thus given by

$$K_i = \sqrt{\frac{\sum K_i^2}{\sum E_i^2}} \cdot E_i$$

and

$$\left(\frac{S}{N}\right)_o = \frac{\left[\sum \sqrt{\frac{\sum K_i^2}{\sum E_i^2}} E_i^2\right]^2}{\sigma^2 \sum K_i^2} = \frac{\sum E_i^2}{\sigma^2} = \frac{\sum A_i^2}{2\sigma^2}$$

This is the optimal (ratio squared) combining formula, and indicates that the weighting $K_i = q E_i$ is the one we want.

Since the IF level in the i^{th} channel is simply $\alpha E_0 E_i = q E_i$, and i^{th} signal is weighted by the correct factor automatically in the SPI combiner scheme.

As noted at the beginning, this analysis is rigorously correct only if the narrowband filter F1 is narrow enough so that no noise is allowed to appear on its output. This condition is in practice quite readily met, because the ratio of the bandwidth of the noise to the bandwidth of the filter can easily be a thousand or so, providing a C/N of $\geq$ 30 db at the output of the i^{th} filter for $\frac{E_i}{\sigma} = 0$ db. The situation is somewhat complicated by noisy oscillator theory, which will be examined further later. The restriction to high S/N is necessary to ensure that the output noise is made up only of input noise and does not have an appreciable component caused by noise on the IF signal. This means that at least one of the input

signal-to-noise ratios be much greater than one, or that if they are equal and in the vicinity of one, n must be large.

DETAILED THEORY OF OPERATION

When we consider the effects of a non-zero value for the bandwidth of filter F1, a lower S/N at the output, and a finite time constant in the AGC, a more detailed analysis is required.

Notation will be as before with an AGC time constant of τ and filter bandwidth of $\frac{b}{2\pi}$. The noise σ has power spectral density No and bandwidth W. We will consider this noise to be a sequence of little wavelets, each with duration $\frac{1}{W}$ and having amplitude and phase independent of all other wavelets. The amplitudes are Rayleigh distributed and the phases are uniformly distributed from $0-2\pi$. This somewhat heuristic approach is useful because since $b \ll W$, each of these wavelets appears as an impulse to filter F1.

Since we are interested in the effects of filter bandwidth and AGC time constant, it makes no difference whether the noise input is taken at the system input or is added in at the point indicated in Figure 4, the amplitude transformation being $\frac{\lambda B}{2}$.

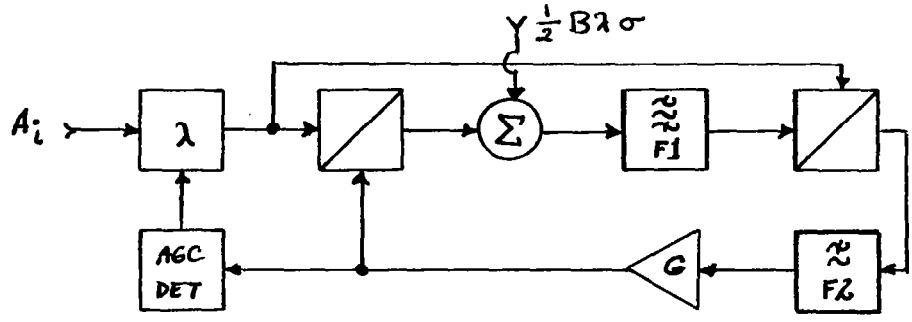

FIGURE 4

As previously observed, this system is an oscillator which the AGC controls to an output level of B. If the input is $A\cos(\omega_i t+\phi)$, and $\sigma=0$, $\lambda=\frac{2}{A\sqrt{G}}$ as before. Now we turn on σ. A wavelet hitting F1 causes an impulse response from F1 which should be a sinusoid with a decaying exponential envelope. This response will be of the form $\delta\frac{b}{2}e^{-\frac{b}{2}t}\cos(\omega_{if}t+\xi)$, where δ is the area under the wavelet, and ξ is the wavelet phase. If we now assume that the AGC time constant, γ, is very large, the loop appears to be an integrator (because of the in-phase feedback configuration), and the response to the wavelet at the output of the filter is $\delta\frac{b}{2}\cos(\omega_{if}t+\xi)$. The succeeding wavelets contribute similar responses, all adding vectorially. As each step is added, a sequence of random steps is generated, resulting in a noisy response having variance that increases linearly with time in both amplitude and phase. These will simply be random walks. The resulting perturbations will have in-phase and quadrature components with respect to the main loop oscillation, and since the noise power spectral density is N_0 over a bandwidth of W, the variance of the in-phase component is $\frac{1}{16}b^2B^2\lambda^2N_0/W$. Thus the variance of the amplitude fluctuation of the signal at the output (since there are W of them in one second) is $\frac{1}{16}b^2B^2\lambda^2\frac{N_0}{W}\cdot\left[\frac{\lambda}{2}A\right]^2W=\frac{1}{64}b^2A^2\lambda^4B^2G^2N_0$ and after time T_0 the mean-squared amplitude fluctuation of the output signal is $\frac{1}{64}b^2A^2\lambda^4B^2G^2N_0T_0$. Since as before, $\lambda=\frac{2}{A\sqrt{G}}$, this is $\frac{B^2b^2N_0T_0}{4A^2}$. In addition, each wavelet contributes a phase perturbation with a mean-square value of approximately

$$\frac{\lambda^2B^2N_0}{4W}\cdot\frac{b^2}{4}\cdot\frac{1}{B^2}=\frac{\lambda^2b^2N_0}{16W}=\frac{b^2N_0}{4A^2GW}$$

and after time T_0 this results in a mean-square phase fluctuation of $\frac{b^2 N_0 T_0}{4A^2 G}$. These results are valid as long as the amplitude fluctuations are small compared with the average amplitude. These mean-square fluctuations will increase without bound until the system becomes non-linear as long as the AGC does nothing to correct them. Therefore, it seems desirable to keep the time constant of the AGC small enough so that $\frac{B^2 b^2 N_0 \gamma}{4A^2} \ll B^2$, or that $\gamma \ll \frac{4A^2}{b^2 N_0}$.

We will now investigate the effect of the AGC time constant on this process.

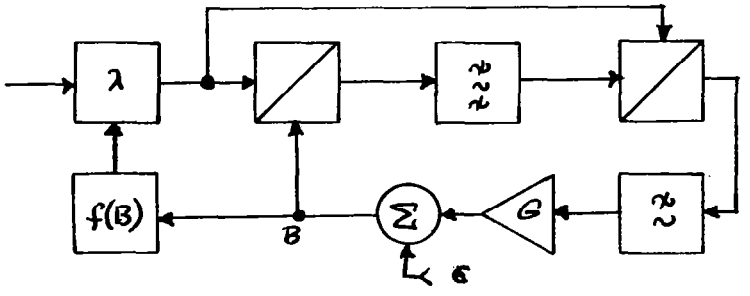

FIGURE 5

ϵ is an additive perturbation at the input to the loop amplifier G. The IF bandwidth $b/2\pi$ is such that its time constant $\frac{2}{b}$ is much less than γ, the time constant of the AGC loop. The loop equation then becomes

$$B = G\left[A^2\lambda^2 B\right] + \epsilon$$

This is the same as a system with the AGC box (λ) relocated:

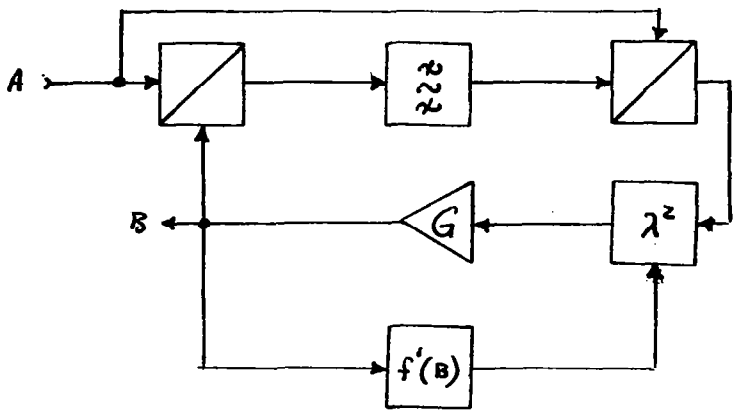

FIGURE 6

If the time constant of the AGC loop $G\lambda^2 f'(B)$ is τ, then the system function of the λ-box in the original block diagram must be of the form $\frac{1}{\sqrt{1+\tau s}}$. This characteristic, incidentally, was found to be essential to the stable operation of the AGC.

The system of Figure 6 will be analyzed, since the positive feedback of B makes the system of Figure 5 difficult. Results, to the approximations we make, should be equivalent.

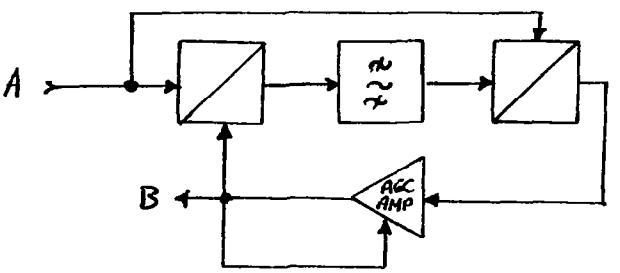

FIGURE 7

The average gain of the AGC amplifier in Figure 7 is $\frac{1}{A^2}$ as expected. Let us denote this as G_0. We then postulate the AGC

amplifier input to be $\alpha\cos(\omega_0 t+\theta)$, plus a small step-type input $\eta\cos(\omega_0 t+\varrho)$. We make the assumption that $\eta \ll \alpha$. The step will be initially multiplied by G_0, but should slowly change the gain of the AGC amplifier in such a way that $\alpha\cos(\omega_0 t+\theta)$ times the change in gain will eventually cancel the component of the step that is in phase with $\alpha\cos(\omega_0 t+\theta)$. The output of the AGC would then be

$$B = G_0\left[\alpha\cos(\omega_0 t+\theta)+\eta\cos(\omega_0 t+\theta)\cos(\theta-\varrho)\right.$$
$$\left.+\eta\sin(\omega_0 t+\theta)\sin(\theta-\varrho)-\eta\cos(\omega_0 t+\theta)\left[1-e^{-t/\tau}\right]\right]$$

It can be seen that the quadrature component of $\eta\cos(\omega_0 t+\varrho)$ is merely multiplied by G_0, while the in-phase component sees the linear equivalent system of Figure 8:

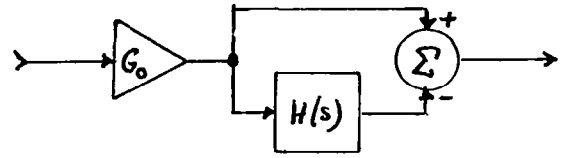

FIGURE 8

Filter $H(s)$ has a bandwidth of $\frac{1}{\pi\tau}$ cps, and a center frequency of ω_0.

If we now identify the perturbing input step amplitude as the noise-caused output of the second modulator, we have $\eta = SA\frac{b\lambda}{4}$ (a factor of $\frac{A\lambda}{2}$ occurs in the mixer) and $\varrho = \varphi$.

The response of the AGC to an impulse at the input to F1 is thus

$$B = GA\lambda\frac{b}{4}e^{-t/\tau}\left[\cos\left(\omega_0+\sqrt{\tfrac{b}{2\tau}}\right)t+\cos\left(\omega_0-\sqrt{\tfrac{b}{2\tau}}\right)t\right]$$

This can be rewritten as

$$B = GA\lambda \frac{b}{2} e^{-t/\tau} [\cos(\omega_0 t)][\cos\sqrt{\frac{b}{2\tau}}\, t]$$

If $\frac{b}{2} \gg \frac{1}{\tau}$, then this waveform is as shown in Figure 9:

FIGURE 9

The beat frequency is $\frac{1}{2\pi}\sqrt{\frac{b}{2\tau}}$ cps, and the integral of the square is $\frac{b^2\tau}{4} \cdot \frac{A^2\lambda^2G^2}{4}$. The noise input shown in Figure 4 thus perturbs the amplitude of the output in the following way. The amplitude of each wavelet is $\frac{1}{2} B\lambda\sqrt{N_0}$. Since 1/2 the power in the noise can be expected to give rise to in-phase responses from F1, the power in the in-phase output fluctuation is

$$\left(\frac{1}{4} B\lambda\sqrt{N_0}\right)^2\left(\frac{b^2}{16} A^2\lambda^2G^2\tau\right) = \frac{1}{128} G^2B^2\lambda^4 N_0 b^2A^2\tau$$

$$= \frac{B^2b^2N_0\tau}{8A^2}$$

The variance of the amplitude of the in-phase output signal fluctuation is then $\frac{B^2b^2N_0\tau}{4A^2}$. This is the same result derived without the AGC, but T_0 has been identified as τ.

Because the perturbation in AGC gain does not affect the quadrature component, it does not affect the phase perturbation of the main oscillation, and thus the result derived previously remains valid. We thus have a mean-square phase fluctuation of $\frac{b^2N_0T_0}{4A^2G}$ accumulating during an interval of duration T_0.

We will analyze the n-channel system for simplicity with equal input signals and equal input noises to each of the channels. The results will be generalized to fit the varying (S/N) situation later. A simplified block diagram is shown in Figure 10.

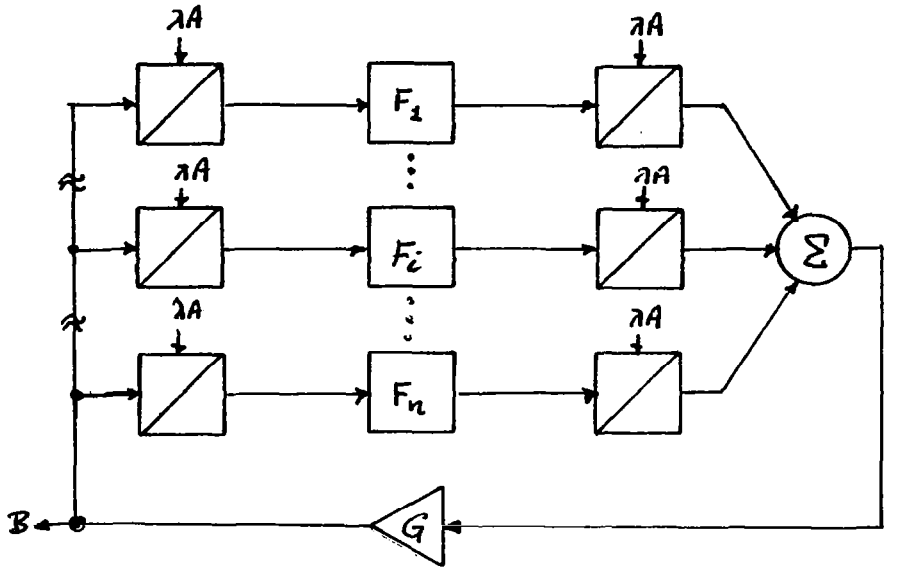

FIGURE 10

In the absence of noise, the output is given by $B = nB\lambda^2A^2G$, and thus to give a loop gain of one,

$$G\lambda^2 = \frac{1}{nA^2}$$

The block diagram can thus be redrawn as shown in Figure 11.

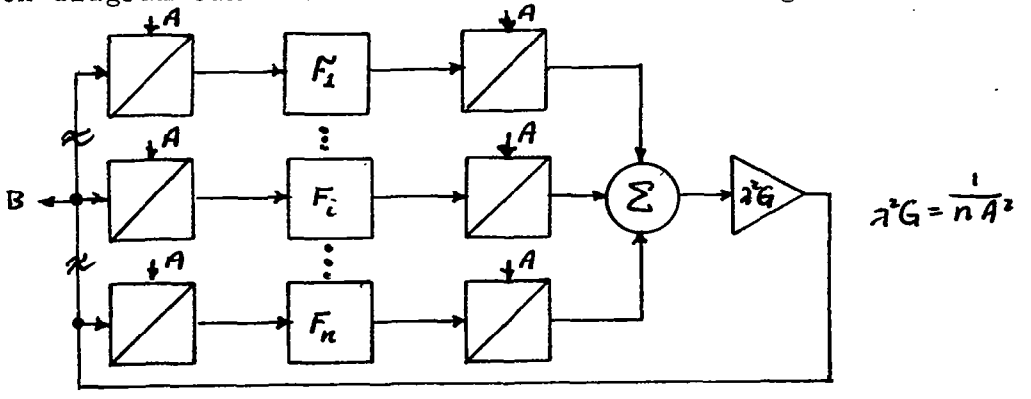

FIGURE 11

If uncorrelated noise is applied to each of the n sets of inputs, two types of perturbation will be produced. First, the noise produces an equivalent noise source at the input of each of the F_i. Second, perturbations are no longer carried around the loop by the basic signal-caused oscillation alone but are also carried by the noise components. This occurs because the portion of the output noise contributed by the i^{th} channel will correlate with the noise input to the i^{th} channel (and only the i^{th} channel) to produce a larger output from F_i than that obtained from the signal correlation alone. The correlation of the random variable gives a factor of two, making the loop gain for this process $2N_0W\lambda^2G$. The system loop gain can then be broken into two paths as shown in Figure 12:

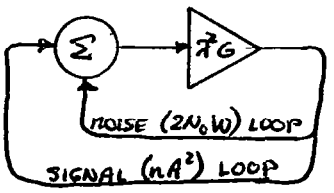

FIGURE 12

The value of λ^2G must now be $\frac{1}{nA^2+2N_0W}$ to maintain a loop gain of one. The flow graph of Figure 13 is now applicable:

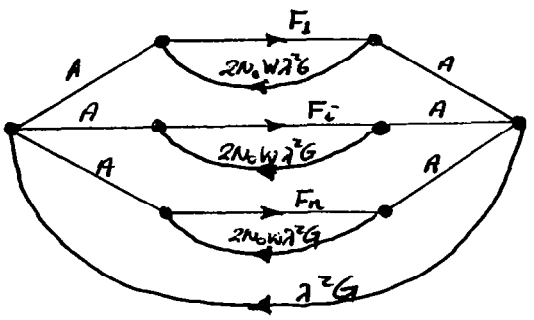

$$\lambda^2G = \frac{1}{nA^2+2N_0W}$$

FIGURE 13

It should be noted that since the noise in each of the channels is uncorrelated with that in any other channel, there are no noise feedback loops from the output of one filter to the input of any other.

The transfer function used for filter F1 is that for a simple RLC filter. Use of a higher order filter should not appreciably change the results of the analysis, however.

$$F(j\omega) = \frac{jb\omega}{jb\omega + (\omega_{1F} - \omega^2)}$$

where $b/2\pi$ is the filter bandwidth and ω_{1f} is the center frequency.

The system (Figure 13) function is then given by

$$H(j\omega) = \frac{jA\frac{b}{2}\omega}{(\omega_0^2 - \omega^2)}$$

This reflects the step nature of the impulse response, and predicts that the impulse response envelope is a step of amplitude $\frac{b}{2}$, having phase relative to the existing oscillation determined by the time of occurrence of the impulse.

The system response to an impulse at the input of F_i consists of two parts. The first is a decaying exponential at the output of F_i due to the response of F_i and its immediate feedback loop. The time constant for this response is

$$\frac{2}{bnA^2}\left[nA^2 + 2N_0W\right]$$

This response then enters the main loop where it feeds all F's equally. The second part of the response consists, therefore, of the responses of all the F's, differing only in the phase angles of the inputs (ϕ_i). We will call this common response to a noise

pulse the "recirculating" noise and the immediate feedback loop response "straight-through" noise.

The "recirculating" noises add up in phase (the ϕ_i are removed by SPI action at the second mixer) and increase exponentially to the amplitude of the output step. Each one of the responses thus increases to $1/n$ of the output step. The sum of the "recirculating" responses increases as fast as the "straight-through" response decreases, thus holding the output constant. In addition, at the output of the excited filter, the maximum value of the "recirculating" noise is $1/n$ the maximum value of the "straight-through" noise.

If we now denote the i^{th} noise pulse input as $J_i(t)\cos(\omega t + \xi_i(t))$, the input signal as $A\cos(\omega t + \phi_i)$, and the IF level (at the output of the filter) as $V_F\cos(\omega t + \phi_i - \theta)$, then the input to F is given by

$$\frac{V_F J_i^2(t)\cos(\omega t + \phi_i - \theta)}{nA^2 + 2N_0W}$$

Notice that this is in-phase with the signal at the output of the filter, and thus produces a step at the output of the system of

$$\frac{\frac{b}{2} V_F A\left[J_i^2(t) - \overline{J_i^2}\right]\cos(\omega t + \theta)}{W\left[nA^2 + 2N_0W\right]}$$

These steps then add to give

$$\sum_i \frac{b}{2} V_F A \frac{\left[J_i^2(t) - \overline{J_i^2}\right]\cos(\omega t + \theta)}{W[nA^2 + 2N_0W]} \qquad (1)$$

A second component of the output noise is caused by the IF level multiplying the noise at the input to the i^{th} second mixer then multiplying by the signal at the input to the j^{th} first

mixer and producing a wavelet at the input to the j^{th} filter of

$$V_F A J_i \cos(\omega t - \xi_i + \phi_j + \phi_i - \theta)$$

After passing through the filter and multiplying with the signal at the second mixer, a step appears at the summation of

$$\frac{\frac{b}{2} V_F A^2 (J_i/W)}{nA^2 + 2N_0 W} \cos(\omega_0 t + \xi_i - \phi_i + \theta)$$

An identical response is obtained from each of the n modules, and thus the output from this cause is

$$\frac{n\frac{b}{2} V_F A^2 (J_i/W)}{nA^2 + 2N_0 W} \cos(\omega_0 t + \xi_i - \phi_i + \theta) \qquad (2)$$

A third source of output noise is a result of the IF level $V_F \cos(\omega t + \phi_i - \theta)$ multiplying with the signal at the second mixer to produce an output from the summation of $nV_F A \cos(\omega t + \theta)$ which then multiplies the noise at the first mixer of the i^{th} channel to give a wavelet input to the i^{th} filter. This produces a step which multiplies with the signal at the second mixer to give a summer output of

$$\frac{n\frac{b}{2} V_F A^2 (J_i/W)}{nA^2 + 2N_0 W} \cos(\omega_0 t - \xi_i + \phi_i + \theta)$$

This perturbation is identical to the previous one is amplitude, but has a phase perturbation of $-\xi_i + \phi_i$ instead of $+\xi - \phi_i$. The resultant of the two will thus be in phase with the main signal output and thus will only give rise to amplitude perturbations.

A fourth source of output perturbation is "cross noise excitation". The IF level multiplies with the noise at the second mixer of the i^{th} channel and then multiplies with the noise at the first mixer of the j^{th} channel. This leaves the j^{th} filter as a step

which then multiplies with the signal at the second mixer to produce an output from the j^{th} channel of

$$\frac{\frac{b}{2}V_F A\,(J_i J_j/W)}{nA^2+2N_oW}\cos(\omega t+\xi_i-\xi_j+\phi_j-\phi_i+\Theta)$$

A corresponding output appears at the output of the i^{th} channel of

$$\frac{\frac{b}{2}V_F A\,(J_j J_i/W)}{nA^2+2N_oW}\cos(\omega t+\xi_j-\xi_i+\phi_i-\phi_j+\Theta)$$

Because of the phase structure, these add to produce only amplitude perturbations of the output. At the summer output we then have

$$\sum_{\substack{i\\ i\neq j}}\sum_{j}\frac{\frac{b}{2}V_F A\,(J_i J_j/W)}{nA^2+2N_oW}\cos(\omega t+\xi_j-\xi_i+\phi_i-\phi_j+\Theta) \qquad (3)$$

These four are the principal sources of output perturbations to the main loop oscillation. The first three types are repeated for each channel. The statistical average of the resultant sum of all these perturbations is zero, and the variance of the amplitude of the steps produced at the output is, for the n steps of the first type,

$$\frac{n\frac{b^2}{4}V_F^2A^2\,(2N_oW/W)^2}{(nA^2+2N_oW)^2}=\frac{nb^2V_F^2A^2N_o^2}{(nA^2+2N_oW)^2}$$

For n steps of the second and third types added together we have

$$\frac{n^3\frac{b^2}{4}V_F^2A^4\,(4N_oW/W^2)}{(nA^2+2N_oW)^2}=\frac{n^2b^2V_F^2A^4N_o}{W(nA^2+2N_oW)^2}$$

For the summation of the fourth type we get a variance of

$$\frac{n(n-1)}{2}\cdot\frac{2\frac{b^2}{4}V_F^2A^2\,(2N_oW/W)^2}{(nA^2+2N_oW)^2}=\frac{n(n-1)\,b^2V_F^2A^2N_o^2}{(nA^2+2N_oW)^2}$$

These three expressions added together then give the variance of the system output produced by the input noises in a duration 1/W, which is

$$\frac{n^2 b^2 V_F^2 A^2 N_0}{W(nA^2+2N_0W)^2}\left[nA^2+N_0W\right] \qquad (4)$$

If $nA^2 \gg 2N_0W$, this simplifies to

$$nb^2V_F^2N_0/W$$

This is the variance of the perturbation of the output signal due to one set of input noise wavelets.

The next set of wavelets multiply the main oscillation plus recirculating noise at the second mixers. The perturbation response is again only an amplitude perturbation with variance differing only slightly with that calculated above. However, the product of the wavelets with straight-through noise at the second mixer produces phase as well as amplitude perturbation at the system output. This latter amplitude variance is small compared with that from the other sources, and can be neglected, but the phase perturbation does remain.

As before, the variance of the signal output increases with time. Since there are T_0W wavelets in time T_0, the output signal amplitude fluctuation has variance

$$\frac{n^2 b^2 V_F^2 A^2 N_0 T_0}{(nA^2+2N_0W)^2}(nA^2+N_0W) \qquad (5)$$

The square of the average output of the system is $(nAV_F)^2$, so the ratio of the output variance to the square of the output signal is

$$\frac{b^2 N_0 (nA^2 + N_0 W) T_0}{(nA^2 + 2N_0 W)^2} \tag{6}$$

If $nA^2 \gg 2N_0 W$, this is

$$\frac{b^2 N_0 T_0}{nA^2}$$

When we include the AGC action in the loop, T_0 becomes τ, and the ratio of the output variance to the square of the output variance becomes

$$\frac{b^2 N_0 \tau}{nA^2}$$

Rewriting this in terms of the ideal output signal-to-noise ratio $\frac{nA^2}{2N_0 W}$, the ratio of the bandwidths of the noise and the filter, and the ratio of the filter and AGC time constants gives

$$\frac{b^2 N_0 \tau}{nA^2} = \frac{2N_0 W}{nA^2} \cdot \frac{b}{W} \cdot \frac{b}{2} \cdot \tau$$

Since $2N_0 W \ll nA^2$, and in general $\frac{b}{W} \ll 1$, if $\frac{b}{2} \cdot \tau$ is small, the output fluctuation will be small. The restriction on τ is thus roughly

$$\tau \ll \frac{2W}{b^2}$$

We now more carefully examine the phase and amplitude perturbations produced by the product of the input noise with the straight-through noise at the second mixer. Because the filter has memory, the IF input to the second mixer is a function of previous noise

inputs, and the equivalent noise input to the filter is a non-linear function of the input noise. For purposes of computing the product of the input noise with straight-through noise at the second mixer, we make little error if we assume that the straight-through noise results from the product of the input noise with the output signal component to provide a noise spectral density at the input to the filter of center height

$$\frac{V_F^2 n^2 A^2 N_o/2}{(nA^2+2N_oW)^2}$$

The product of the noise component of the output with the signal input gives a noise spectral density with center height of approximately

$$\frac{V_F^2 n A^2 N_o/2}{(nA^2+2N_oW)^2}$$

Since this is $\frac{1}{n}$ of the first component, it will be ignored.

The product of the output noise with the input noise gives a spectral density with center height of

$$\frac{V_F^2 n N_o^2 W}{(nA^2+2N_oW)^2}$$

adding this to the first component gives

$$\frac{n V_F^2 N_o}{2(nA^2+2N_oW)}$$

The straight-through noise power at the output of the filter is then the above multiplied by the area under the magnitude of the system function of the filter with its self loop. We thus have a straight-through noise power of $\frac{V_F^2 N_o b}{4A^2}$. The signal power is $\frac{V_F^2}{2}$, so if $N_o b \ll \frac{A^2}{2}$, the error caused by assuming the

IF level to be V_F only is not large. If we now use $\frac{V_F^2 N_0 b}{4A^2}$ as the power of a random carrier at the second mixer, we can now complete equivalent noise inputs to the filter resulting from the product of straight-through noise and input noise. It should be noted that since $\frac{V_F^2 N_0 b}{4A^2} \ll \frac{V_F^2}{2}$ the variance of the output amplitude perturbations from this source will be small compared with those computed previously. If $\frac{V_F}{2A}\sqrt{N_0 b}$ is used instead of V_F in the equations used to compute the amplitude variance, a new set of equivalent noise wavelet inputs to the filter can be obtained. The resulting part of the step response in quadrature with the main oscillation has amplitude variance of approximately

$$\frac{n^2 b^3 \gamma_P^2 N_c^2 / W}{8(nA^2 + 2N_0 W)}$$

The variance of the phase perturbation is obtained by dividing this by the square of the output amplitude $n^2 V_F^2 A^2$ to give, for one wavelet input,

$$\frac{b^3 N_0^2}{8A^2 W(nA^2 + 2N_0 W)}$$

Since there are $T_0' W$ wavelets in time T_0', the variance of the phase perturbation accumulated in this time is

$$\frac{b(N_0 b)^2 T_0'}{8A^2(nA^2 + 2N_0 W)}$$

If $nA^2 \gg 2N_0 W$, this is essentially

$$\left(\frac{N_0 b}{A^2}\right)^2 \cdot \frac{b T_0'}{8n}$$

Thus, the time required for the standard deviation of the phase perturbation of the output signal to reach 2π is approximately

$$T_{2\pi} = \frac{32n}{b}\left(\frac{A^2}{N_0 b}\right)^2 \pi^2$$

This can be rewritten as

$$T_{2\pi} = \frac{32\pi^2}{b} \cdot \frac{nA^2}{2N_0 W} \cdot \frac{A^2}{N_0 b} \cdot \frac{W}{b}$$

AGC operation under the noisy condition is somewhat more complicated than the previously treated case. Assume the IF signal at the output of the i^{th} filter is $V_F \cos(\omega t + \phi_i - \theta)$ plus a perturbation $c_i(t)\cos(\omega t + \gamma_i(t))$. Assume also that the response of the AGC system ($\mathcal{F}^{-1}G$ in Figure 11) to an input $z(t)$ is

$$\frac{Kz(t)}{[H(z^2(t)]^{1/2}}$$

where K is a constant and $H(z^2(t))$ denotes the output of a narrow-band low pass filter acting on $z^2(t)$. We then define $\bar{z}(t) = [H(z^2(t)]^{1/2}$ Suppose $z(t)$ is perturbed by a function $\mu(t)$. Then the AGC output is given by

$$\frac{K(z(t)+\mu(t))}{\left[H\left(z^2(t)+2\mu(t)z(t)+\mu^2(t)\right)\right]^{1/2}} \approx \frac{K\,(z(t)+\mu(t)}{\left[H\left(z^2(t)+2\mu(t)z(t)\right)\right]^{1/2}} \approx K\left[\frac{z(t)}{\bar{z}(t)} + \frac{\mu(t)}{\bar{z}(t)} - \frac{z(t)}{\bar{z}(t)} \cdot \frac{H(\mu(t)z(t))}{\bar{z}^2(t)}\right]$$

Note that $H(\mu(t)z(t))/\bar{z}(t)\bar{z}^2(t)$ is the change in AGC gain due to the input perturbation. $H(\mu(t)z(t))/\bar{z}(t)$ is the response of the low pass filter to the envelope of the component of the perturbation that is in phase with $z(t)$. Applying this to the case to be analyzed,

$$z(t) = nV_F A\cos(\omega t + \theta) + V_F \sum_i J_i(t)\cos(\omega t + \xi_i(t) - \phi_i + \theta)$$

and thus

$$\bar{z}^2(t) = \frac{nV_F^2}{2}\left(nA^2 + 2N_0 W\right)$$

Also,

$$\mu(t) = \sum_i \left[A c_i(t) \cos(\omega t + \phi_i - \psi_i(t)) + J_i(t) c_i(t) \cos(\omega t + \xi(t) - \psi_i(t)) \right]$$

Thus

$$H(\mu(t) z(t)) \approx \frac{V_F}{2} (nA^2 + 2N_0W) H\left[\sum_i c_i(t) \cos(\phi_i - \psi_i(t) - \theta)\right]$$

and thus

$$\frac{H(\mu(t) z(t))}{\bar{z}^2(t)} \approx \frac{1}{nV_F} H\left[\sum_i c_i(t) \cos(\phi_i - \psi_i(t) - \theta)\right]$$

When we absorb $\frac{1}{\bar{z}(t)}$ into the constant K, the AGC correction becomes

$$K \bar{z}(t) \frac{H(\mu(t) z(t))}{\bar{z}^2(t)} =$$

$$K\left[\cos(\omega t + \theta) + \frac{1}{n}\sum_i J_i(t) \cos(\omega t + \xi_i(t) - \phi_i + \theta)\right]\left[H\left(\sum_i c_i(t) \cos(\phi_i - \psi_i(t) - \theta)\right)\right]$$

Thus, the linear system seen by perturbations at the input to the second mixer is that of Figure 13 with

$$\lambda^2 G = \frac{1}{nA^2 + 2N_0W}\left[1 - \frac{jb\omega}{jb\omega + (\omega_0^2 - \omega^2)}\right]$$

for the component of the perturbation in phase with the main oscillation, and with

$$\lambda^2 G = \frac{1}{nA^2 + 2N_0W}$$

for the quadrature component. This describes the same system as shown in Figure 7, and thus the previous results are valid.

The linearized AGC model is valid only for $|c_i(t)| \ll V_F$. If this condition is not met, the terms $V_F J_i(t)\cos(\omega t + \xi_i(t) - \phi_i + \theta) + c_i(t) J_i(t)\cos(\omega t + \xi_i(t) - \gamma(t))$ will not be treated by the AGC as described. However, as long as $nA^2 \gg 2N_0W$, the system output S/N should be favorable, even if $\frac{N_0 b}{A^2} > 1$.

If we now remove the restriction that the input signals are identical in amplitude, the analysis is changed in the following ways.

Assume the input signals are given by $A_i \cos(\omega_i t + \phi_i)$ and input noise powers are N_0W. The gain of the feedback loops in Figure 13 are changed to be

$$\lambda^2 G = \frac{1}{\sum_i A_i^2 + 2N_0W}$$

The IF level V_F is now not identical in the various channels and must be given by

$$V_{Fi} = \frac{A_i B}{\lambda [\Sigma A_i^2 G]^{1/2}} = \frac{A_i B}{\Sigma A_i^2 (\Sigma A_i^2 + 2N_0W)^{1/2}}$$

When this is included in the summations of equations (1), (2), and (3), equation (4) becomes

$$\frac{(\Sigma A_i^2)^2 B^2 b^2 N_0 (\Sigma A_i^2 + N_0W)}{W(\Sigma A_i^2 + 2N_0W)^3}$$

Equation (5) is now

$$\frac{(\Sigma A_i^2)^2 B b^2 N_0 (\Sigma A_i^2 + N_0W) T_0}{(\Sigma A_i^2 + 2N_0W)^3}$$

and equation (6) becomes

$$\frac{b^2 N_0 (\Sigma A_i^2 + N_0W) T_0}{(\Sigma A_i^2 + 2N_0W)^2}$$

Again, if $\sum A_i^2 \gg 2N_oW$, this is

$$\frac{b^2 N_o T_o}{\sum A_i^2}$$

A similar process gives a revised estimate of the phase perturbation.

The results of the analysis are as follows. For output S/N much greater than one, noise at the inputs produces perturbations in both the amplitude and phase of the output. The ratio of the variance of the output amplitude perturbation to the square of the output amplitude is approximately given by

$$\frac{b^2 N_o \gamma}{\sum A_i^2} = \left(S/N\right)_o^{-1} \left(\frac{b}{W}\right)\left(\frac{b}{2} \cdot \gamma\right)$$

Where $(S/N)_o$ is the signal-to-noise ratio after combining, $(\frac{b}{2} \cdot \gamma)$ is the ratio of the time constant of the AGC to the time constant of the filter, and b/W is the ratio of the bandwidths of the filter and the input noise.

The variance of the phase of the output accumulates in a time T_o to a value of

$$\frac{1}{32} b T_o \left(\frac{(\sum A_i)^2}{\sum A_i^2}\right)\left(\frac{b}{W}\right)^2\left(\frac{2N_oW}{\sum A_i^2}\right)^2 \text{ radians}$$

Where $\frac{bT_o}{2}$ is the ratio of the accumulation of time to the time constant of the filter, and $(\sum A_i)^2/\sum A_i^2$ is the SPI combiner improvement factor.

We will now examine the restriction $\sum A_i^2 \gg 2N_oW$. As long as we can specify that the IF filter bandwidth is narrow enough so that only the spike (correlated) part of the input spectrum passes through and that the part of the continuous spectrum that is passed

is negligible, the noise from one channel does not affect any other channel in any way, eliminating the cross-correlation, recirculating, and straight-through noises.

Assume only one input has a signal $A_i \cos(\omega_i t + \phi_i)$, but all inputs have equal but uncorrelated noise $N_o W$. Further, assume $A_i^2 < 2N_o W$. The i^{th} loop will oscillate, giving a system signal output of $KA_i \cos(\omega_o t + \Theta)$ and noise $K\sqrt{N_o W}$. No other loop will oscillate, since the loop gain of any other loop will be less than one because of the AGC action. This is true because the loop gain for the j^{th} loop is given by

$$G_{Lj} = \frac{A_j^2 + 2N_o W}{\sum_i A_i^2 + 2N_o W}$$

If only one of the A_j is non-zero, this expression is one only for that loop. For other than equal noise inputs, a restriction on this analysis is

$$A_i^2 > 2(N_j - N_i)W \quad \text{for any } j$$

It can be seen that if no signal inputs were present, only the loop with the highest noise input would oscillate, and thus that noise would be the only output. Since no other input would correlate with the output, no IF level would be present in the other narrow filters, and no contribution from those channels would appear in the output.

Because the filter is not infinitely narrow, some cross-correlation, recirculating, and straight-through noise is always present. If the noise output from the multiplication of the IF

level from these sources with the other input noises is to be maintained negligible compared to the single channel output, the filter bandwidth restriction is

$$b \ll \frac{W}{n}$$

Returning to the case of $\sum A_i < 2N_oW$, if we assume that the only input, A_i, is causing the loop to oscillate to the exclusion of all other channel input noises, and we introduce a small input A_j in the j^{th} channel, a spike will occur in the j^{th} IF filter because of the correlation of the j^{th} input (no matter how small) with the previously existing output. This IF level will cause the j^{th} channel to contribute to the output, and the two will add up in a ratio-squared manner. It appears obvious that the process can be extended to n channels, thus obtaining the result that as long as $b \ll \frac{W}{n}$ and $\sum A_i^2 > 2W|N_j - N_k|$ for any values of j and k, that the output of the system will be a ratio-squared sum of the inputs, thus giving optimal combining. The results for phase and amplitude fluctuations previously derived are obviously not applicable, but should be of similar form.

In practice, it is expected that as S/N is lowered a threshold will be reached where because of the noise perturbations on the IF signals the combining will not be in-phase. This point will be difficult to measure, and can be said to represent no limitation to system performance, since $b \ll \frac{W}{n}$ is not difficult to achieve unless n is in the hundreds. The threshold point is probably not reached until the inputs fall to

$$\sum A_i^2 \approx 2\left(\frac{b}{W}\right)(N_oW)$$

The results of the theoretical investigation of an n-channel regenerative SPI combiner are the following.

1) Under the assumptions that the filter bandwidth $b \ll \frac{W}{n}$, $\sum A_i^2 > 2W|N_j - N_k|$ for any j and k, and $\sum A_i^2 \gg 2(\frac{b}{W})(N_0 W)$; and that the input noise powers are close to being equal, the SPI system will act as an optimal ratio-squared combiner.

2) The output signal will be shifted in frequency and the (DC) value of its phase will be independent of that at the input.

3) If the inputs are given by $A_i S(t) \cos(\omega_i(t) + \gamma(t) + \phi_i)$, where $\overline{S(t)^2} = 1$, the output will be $K S(t) \sum A_i^2 \cos(\omega_0 t + \gamma(t) + \theta)$; where K is some gain constant for the system.

4) If the input signal-to-noise ratio is given by $(S/N)_i = \frac{A_i^2}{2N_0 W}$, where $N_0 W$ is the noise power in the system bandwidth W, the output signal-to-noise ratio is $(S/N)_o = \frac{1}{2N_0 W} \sum A_i^2$.

The noise in the SPI regenerative loop will cause amplitude and phase fluctuations on the output. If the inputs are further constrained so that $\sum A_i^2 \gg 2N_0 W$ (this is equivalent to assuming high signal to noise at the output), the ratio of the amplitude fluctuation variance to the square of the output signal is given by $\frac{2N_0 W}{\sum A_i^2} \cdot \frac{b}{W} \cdot \frac{b}{2} \cdot \tau$, and the variance of the output phase accumulates in time T_0 to a value of

$$\frac{1}{32} b T_0 \left(\frac{(\sum A_i)^2}{\sum A_i^2}\right)\left(\frac{b}{W}\right)^2 \left(\frac{2N_0 W}{\sum A_i^2}\right)^2 \text{ radians.}$$

If $(\frac{b}{W})(\frac{b}{2}\cdot\tau) \ll 1$, which is the general situation, then the amplitude variance is small compared to the output noise $\sqrt{N_0 W}$. Detection errors will thus not be primarily dependent on amplitude fluctuation, but will almost entirely be caused by output noise.

For an evaluation of the effect of the phase perturbation, we will refer to the rms frequency deviation of the output. This is given by $\Delta = \frac{\sum A_i}{4}\left(\frac{2N_0 W}{\sum A_i^2}\right)\left(\frac{b}{W}\right)\sqrt{\frac{b/2}{\sum A_i^2}}$. If all inputs are identical, this is $\Delta = \frac{2N_0 b}{nA^2}\cdot\sqrt{\frac{nb}{32}} = \frac{2N_0 W}{nA^2}\left(\frac{b}{W}\right)\sqrt{\frac{nb}{32}}$. Since $\frac{2N_0 W}{\sum A_i^2} \ll 1$, and $\frac{b}{W} \ll 1$, unless nb is very large, this figure is also very small.

If a system is designed to operate at an output SNR of 20 db, with a bandwidth W of 10 mc and with n=4, the RMS deviation on the output will be less than 1 cps rms if the bandwidth of the IF is less than two megacycles. This is far wider than would be used in a practical system. RMS deviation on the output is thus no problem.

For the same example, if the AGC time constant were $\tau = 0.01$ sec, then to make amplitude variance negligible (< 0.1) compared to output noise requires an IF filter bandwidth of less than 14 kc. This is feasible if a crystal filter is used, and for most systems this would be the approach taken.

The SPI regenerative predetection combiner can thus be expected to give ratio-squared combining of IF input signals with negligible degradation, for a wide range of input SNR's if the IF filter is sufficiently narrow.

Figure 14 shows the predicted ratio-squared combining gain for an n=2 system as the ratio A_1/A_2 is varied.

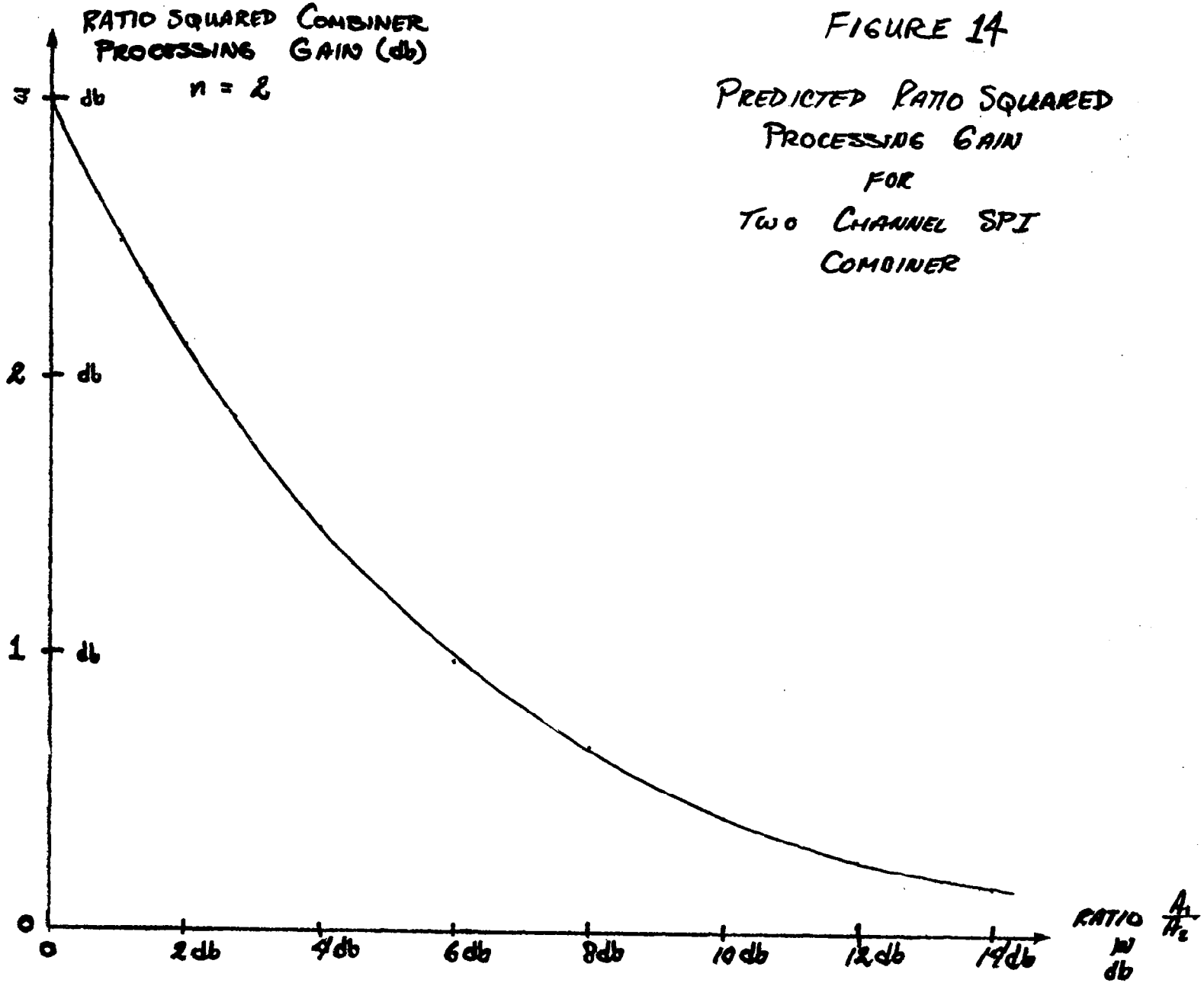

FIGURE 14

PREDICTED RATIO SQUARED PROCESSING GAIN FOR TWO CHANNEL SPI COMBINER

SYSTEM DESIGN AND EXPERIMENTAL RESULTS

The SPI system that was constructed and tested was essentially that analyzed. An input frequency of 70 MHz was chosen to make the system compatible with source equipment utilizing a 70 MHz IF output. A bandwidth of 10 MHz was desired.

Proper SPI action is quite dependent on having a product-type characteristic in both modulators. This is very difficult to achieve with a high degree of linearity and balance, and to alleviate the spurious problem, the output and IF frequencies were carefully chosen.

The first modulator multiplies the 65 - 75 MHz input (f_i) and the output (f_o) to give the IF. The outputs that can arise from this modulation are of the form $nf_i + mf_o$, (n, m=0, ±1, ±2, etc.) and must not fall within the narrow band IF filter unless n=±1, m=±1. Thus

$$nf_i + mf_o \neq f_{if} \quad , \quad |n|, |m| \neq 1$$

The second modulator multiplies the IF and the input to give the output. Frequencies produced here are of the form $pf_i + qf_{if}$ $(p, q = 0, \pm1, \pm2, \ldots)$ and thus

$$pf_i + qf_{if} \neq f_o \qquad |p|, |q| \neq 1$$

These limitations must hold over the bandwidths of f_i and f_o, not merely for individual values.

It is desirable to make the IF frequency lower than the output frequency to prevent any harmonic of the output form falling into the IF and also to allow the use of a crystal filter by keeping the IF below 30 MHz. A frequency plan that allows this is shown in Figure 15.

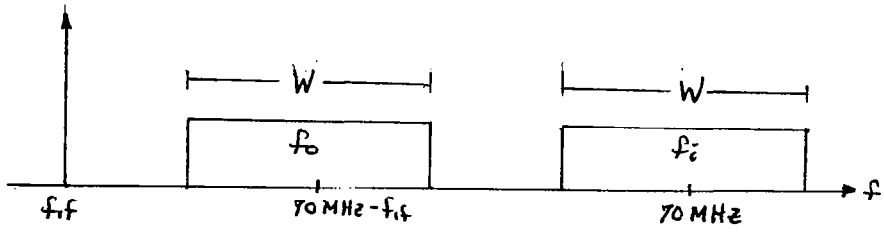

FIGURE 15

We will now attempt to maximize bandwidth while making sure no interference occurs. The limits on the input frequency f_i are given by

$$70\,MHz - W/2 < f_i < 70\,MHz + W/2$$

The limits on the output frequency f_o are

$$70\,MHz - f_{if} - W/2 < f_o < 70\,MHz - f_{if} + W/2$$

To prevent overlap,

$$70\,MHz - W/2 > 70\,MHz - f_{if} + W/2$$

or $$f_{if} > W$$

Also, $$f_{if} < 70 - f_{if} - W/2$$

so

$$W < f_{if} < 35\,MHz - W/4$$

In order to take care of the spurious problem, f_{if} can be arranged so that its harmonics fall between f_i and f_o, or above f_i. Thus

$$70\,MHz - f_{if} + W/2 < 2F_{if} < 70 - W/2$$

and a new lower limit for f_{if} is

$$\frac{70\,MHz}{3} + \frac{W}{6} < f_{if}$$

If we now maximize W, from the above equations, we obtain

$$W = f_{if}$$

and

$$f_{if} < 35\,MHz - f_{if}/4, \text{ or } f_{if} < 28\,MHz$$

but

$$\frac{70\,MHz}{3} + \frac{f_{if}}{6} < f_{if}, \text{ so } f_{if} > 28\,MHz$$

thus

$$f_{if} = 28\,MHz, \text{ and } W < 28\,MHz$$

If W=10 MHz is chosen to permit guard bands and to alleviate the filter problem, the system frequencies are

$$65\,MHz < f_i < 75\,MHz, \quad 37\,MHz < f_o < 47\,MHz, \quad f_{if} = 28\,MHz$$

The frequency diagram will thus be

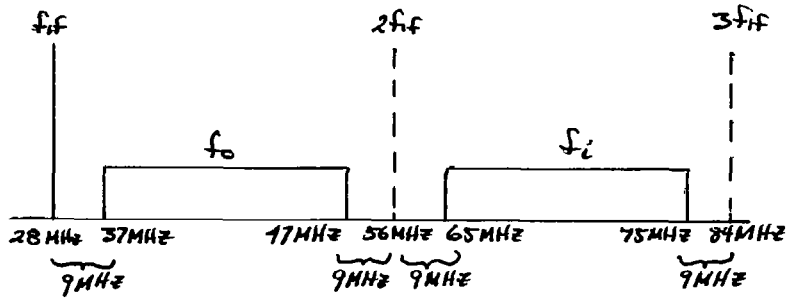

FIGURE 16

In order to permit the use of the combiner over a wide range of input levels, a wide range AGC is necessary. In the analysis section of this report, the AGC attenuator is shown acting on the input signal before it reaches either of the modulators. This means that the modulators will always be operated at a reasonably well defined level; changes from nominal being caused only by the distribution of input levels, and not be their magnitudes. Dynamic range is thus considerably increased.

Optimal SPI performance is predicated on the existence of a perfect correlation at the first mixer. If the second modulator, the second filter, and the output amplifier have a delay τ_d, the correlation process will be adversely affected. In general, for sinusoidal inputs, the amplitude of the correlation coefficient will be multiplied by $\cos(2\pi f_0 \tau_d)$, and is thus a function of input frequency.

One simple, yet effective, way to eliminate this problem is to place a delay $\tau_c = \tau_d$ in the input side of the first mixer, thus having the input and output signals arriving at the mixer at the same time, producing maximum correlation. An attendant requirement on the IF system is that the phase shift through it plus $\tau_c \omega_{if}$ add up to $2n\pi$ to give an IF signal of the proper phase at the second modulator.

Figure 17 shows the block diagram of the system to be built. The system was divided into three separate types of units. The input signal proconditioner and SPI processor must be repeated for each channel, while only one combiner is needed. An n=2 system

was chosen to simplify instrumentation, alignment, and measurement. It was felt that a demonstration for n=2 would give a good indication of the capabilities of an SPI combiner. The system of Figure 17 shows separate signal and noise inputs to each channel for testing purposes. The noise input is equipped with a filter to limit noise bandwidth.

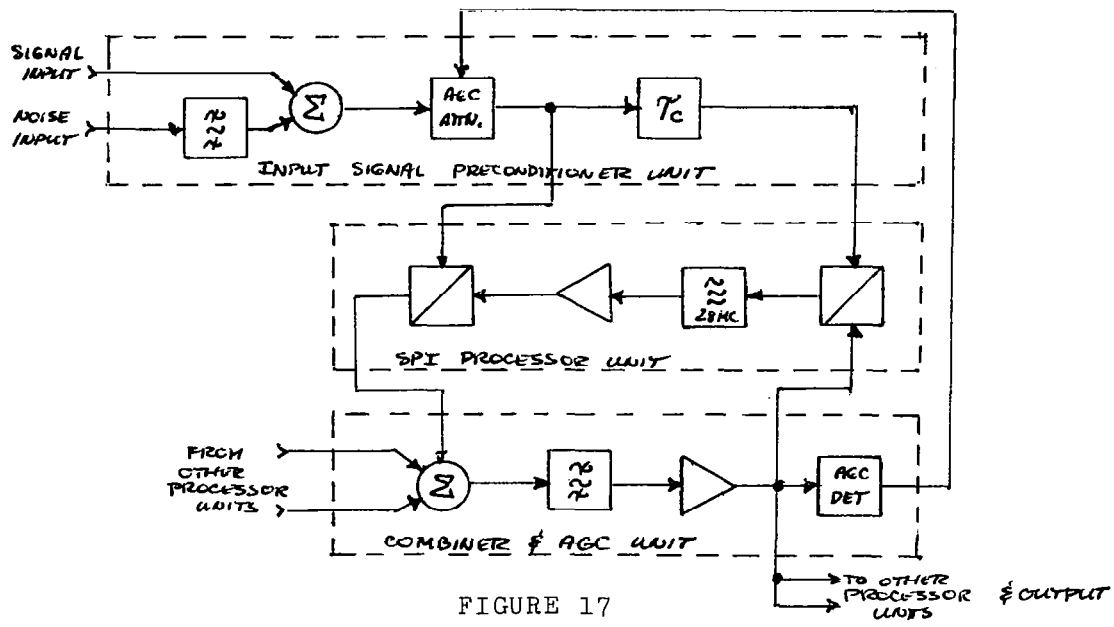

FIGURE 17

The noise filter could have a variable bandwidth to allow adjustment of the noise parameters. Minor deviations from flat frequency response will not be troublesome. The AGC attenuator should have flat frequency response and be voltage controlled over at least a 10 db range.

The modulators should have a very linear multiplicative action over a dynamic range of 30 db at each input (60 db at the modulator output). The frequency response is to be flat for an output

of 37 - 47 MHz (one input 65 - 75 MHz, the other 28 MHz) and for an output of 28 MHz (one input 65 - 75 MHz, the other 37 - 47 MHz).

The 28 MHz narrow band filter is to be very narrow and have at least 30 db of rejection at 37 MHz to minimize spurious signals. A single section crystal filter is thus indicated. A means of trimming the exact center frequency is necessary to match channels. The 28 MHz amplifier can be grouped with the filter and must provide sufficient gain to give adequate IF level to the second modulator.

The combiner (summation) is to provide linear addition of the inputs.

The 37 - 47 MHz filter chooses the lower sideband out of the second modulator. It should be flat (0.5 db) across the 10 MHz band and should reject 28 MHz by at least 60 db and 56 MHz and above by 50 db.

The 37 - 47 MHz output amplifier is to have enough gain to give a useful output and to drive the first modulator. A capability of driving several 75 ohm loads is necessary here.

All system interfaces were chosen to be 75 ohms in keeping with other equipment.

The system was designed to operate with a nominal input level of -6 dbm and an output level of -20 dbm.

The modulators appeared to be the most difficult items to design, and it was necessary to evaluate their conversion loss, balance,

and linearity characteristics before assigning values to levels, gains, and filter rejections in the system.

The linear product-type modulator was designed to give an output of KA(t)B(t) where A(t) and B(t) are the inputs. Spurious outputs and the leakage of A(t) and B(t) were to be fairly low.

A multi-grid vacuum tube can be used for this purpose, but it was decided to try to use a solid state device. A field-effect transistor has a dynamic drain-to-source conductance (G_{ds}) that is a strong function of gate-to-source bias if the drain-to-source voltage is kept below the knee in the characteristics. Figure 18 shows a typical family of FET curves:

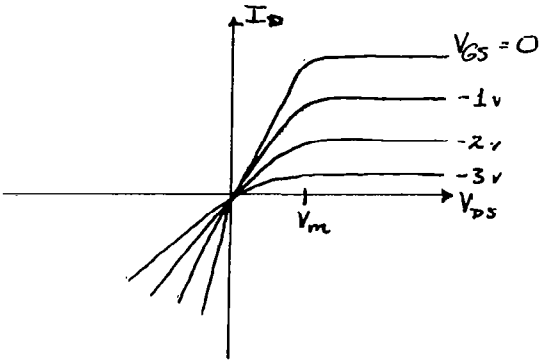

FIGURE 18

If the peak V_{DS} voltage is kept below V_m, the conductance of the FET is as shown in Figure 19:

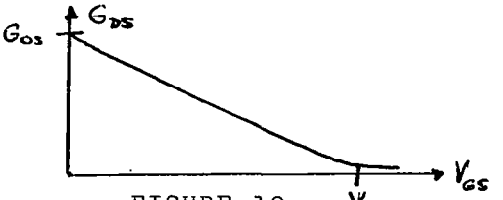

FIGURE 19

An equation that fits this curve for $V_{GS} < V_P$ is

$$G_{DS} = G_{OS}\left[1 - \frac{V_{GS}}{V_P}\right]$$

A modulator that utilizes this characteristic is the balanced configuration of Figure 20:

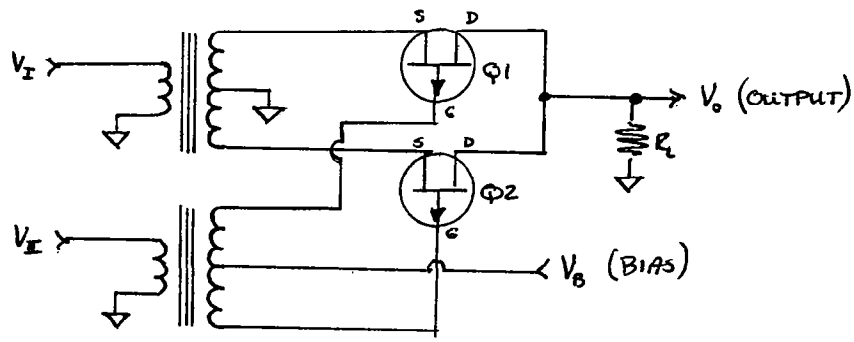

FIGURE 20

The conductance of Q1 will be given by

$$G_{Q1} = G_{OS}\left[1 - \frac{V_B}{V_P} - \frac{V_{II} - V_I}{V_P}\right]$$

and for Q2,

$$G_{Q2} = G_{OS}\left[1 - \frac{V_B}{V_P} + \frac{V_{II} - V_I}{V_P}\right]$$

then,

$$V_o = R_L G_{OS}\left[(V_I - V_o)\left(1 - \frac{V_B}{V_P} - \frac{V_{II} - V_I}{V_P}\right) + (-V_I - V_o)\left(1 - \frac{V_B}{V_P} + \frac{V_{II} - V_I}{V_P}\right)\right]$$

$$= \frac{2R_L G_{OS}}{V_P} \cdot \frac{-V_I V_{II} + V_I^2}{1 + 2R_L G_{OS}\left(1 - \frac{V_B}{V_P}\right)}$$

If we select, for maximum dynamic range, $V_B = V_P/2$, and ignore the V_I^2 term, this becomes

$$V_o = -\frac{2R_L G_{OS}}{V_P(1 + R_L G_{OS})} V_I V_{II}$$

Balance in this modulator is dependent on the degree of balance in the transformers and on the matching between field-effect transistors. If each input can be adjusted for balance, the modulator can be very accurately balanced. In the final design, no attempt was made to balance the 67 - 75 MHz input. This is the signal used for V_I. The V_I^2 output and V_I leak were sufficiently out of band of all filters to be no problem.

In choosing the proper FET, frequency range was quite important. The capacitance between gate and source is the limiting factor, as the effect of capacitance from drain-to-source is cancelled in the second unit. High frequency devices (70 MHz f_T) were used, and the gate-source capacitance tuned out with an inductor across R_L.

To maximize output for a given value of R_L, V_P must be minimized. G_{os} is approximately equal to g_m.

There is therefore, a compromise in selection of the proper FET. A high value of f_T is not compatible with high g_m and low V_P. The best compromise that has been found to date is the 2N2606, which is manufactured by several suppliers.

A transformer was available for the 65 - 75 MHz band having a 75 ohm input impedance and approximately 500 ohms output impedance, center tapped. No transformer, however, was available for the 37 - 47 MHz band, so a balanced output amplifier was designed to provide the necessary phase splitting.

Figure 21 shows the complete schematic for the modulator. The emitter-follower stage permits a high value for R_L, giving a higher conversion efficiency.

Figure 22 shows frequency response, and Figure 23 shows linearity. Notice that for linear operation both inputs should be kept to less than 0 dbm. Notice also that the output is given by

$$V_o(\text{dbm}) = V_I(\text{dbm}) + V_{II}(\text{dbm}) - 20 \text{ dbm}$$

With the parameters of the FET modulator well defined, it was then possible to assign levels and specifications to the remaining system elements. Figure 24 shows the system levels and the amplifier gains required.

The AGC attenuator must have a loss between 0 and 20 db (centered at -6 db) followed by an amplifier to boost the signal back to -6 dbm. The signal is then split, the high level side feeding the second modulator. The large attenuation (12 db) in the delay line leg of the splitter is to provide isolation between the two outputs.

The 28 MHz IF strip must have 54 db of gain total, while the output filter and amplifier must have a gain of 15 db total.

It should be noted that only one channel is shown feeding the summation point. If a second channel were added, the AGC would act to center at -9 db, and all levels prior to the summation would drop 3 db. The level at the output of the second modulator would drop 6 db, but two channels adding up in the summer would regain the 6 db.

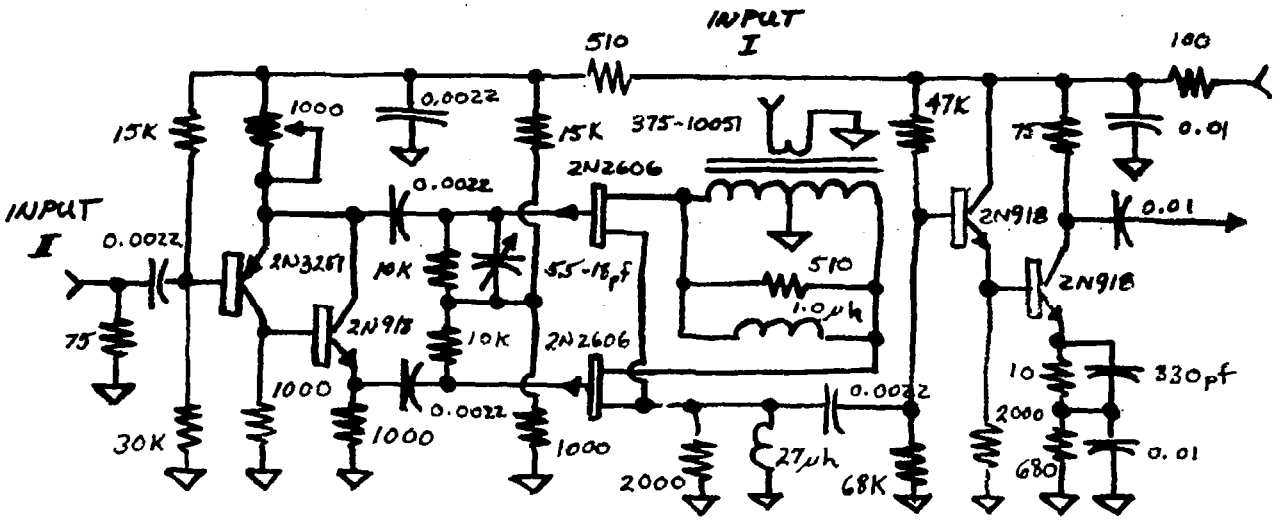

F.E.T. MODULATOR SCHEMATIC
FIGURE 21

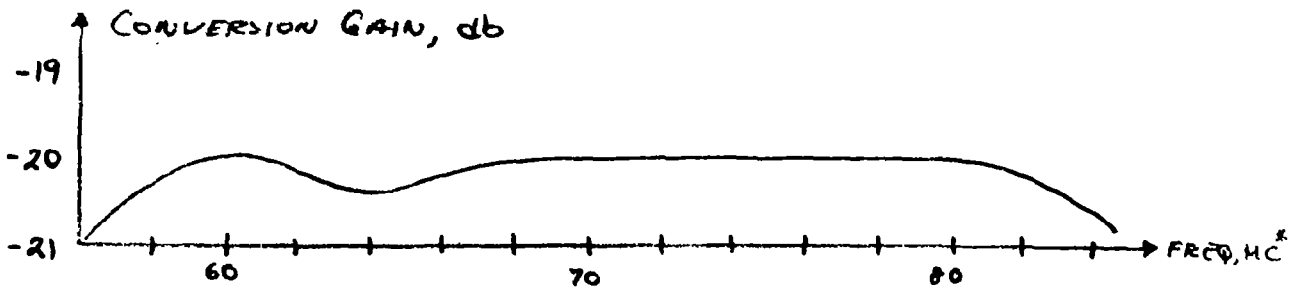

MOD. CONVERSION GAIN VS FREQUENCY
FIGURE 22

* AT INPUT I. 28 MC AT INPUT II AT 0 dbm

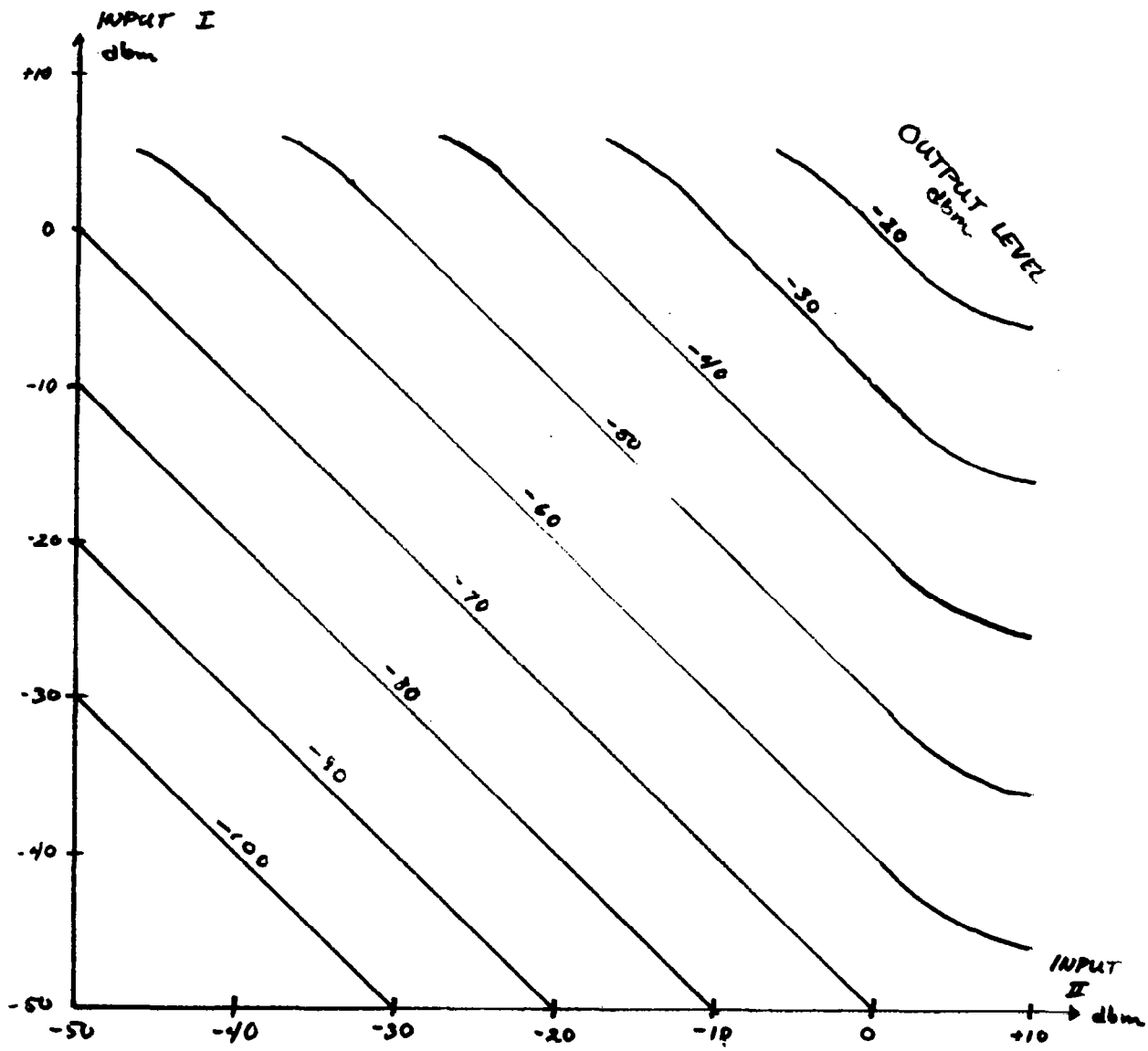

CURVES OF CONSTANT OUTPUT
FOR THE
F.E.T. MODULATOR
FIGURE 23

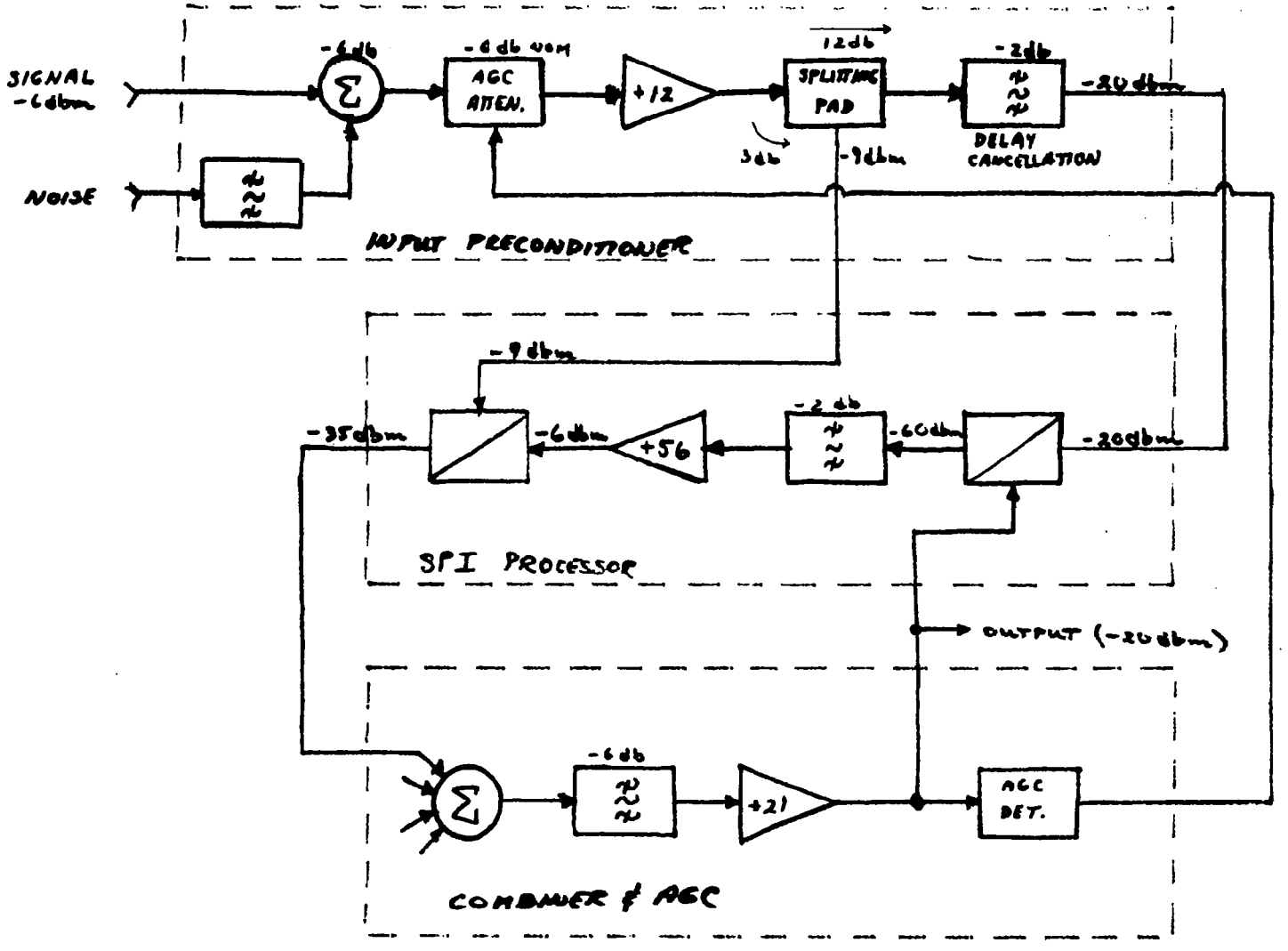

FIGURE 24 LEVEL ASSIGNMENT IN SPI DESIGN

The AGC detector must act so as to maintain the output level at -20 dbm.

The 28 MHz narrow band filter was incorporated into the 28 MHz amplifier. A 28 MHz fundamental mode AT-cut crystal was used in the series mode as the basic filter element. It was driven from a low impedance emitter-follower stage and worked into a 56 ohm load. An inductor was used in parallel to tune out the crystal parallel capacitance, and a trimmer capacitor was placed in series to adjust the exact frequency of operation. The 28 MHz amplifier was made up of five stages, some tuned in the emitter, some in the collector. Gain is 54 db from the input to output measured at 28 MHz. Figure 25 shows the schematic for the filter and amplifier, and Figure 26 shows frequency response.

The combiner makes a voltage summation of its inputs. This unit was designed to accept four inputs, so that without modification an n=4 SPI combiner could be built. The combiner is a single stage feedback amplifier, with the feedback providing a summation node at the transistor base.

The output bandpass filter is to be flat (within 0.5 db) over 37 - 47 MHz, and is to reject 28 MHz by more than 60 db and frequencies above 56MHz by more than 50 db. To meet these requirements, a cascaded high pass - low pass filter with buffering between stages and at the output was designed. The schematic for the combiner and filter is shown on Figure 27, and the filter response is shown on Figure 28.

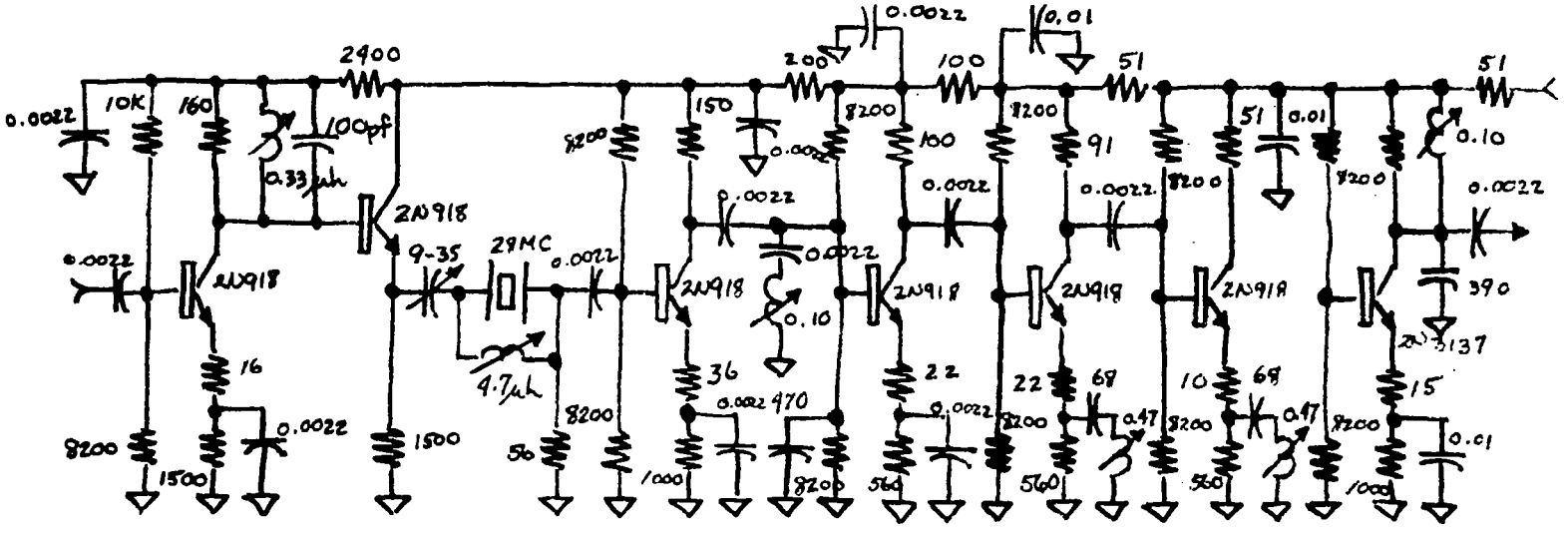

FIGURE 25 28 MC FILTER & AMPLIFIER SCHEMATIC

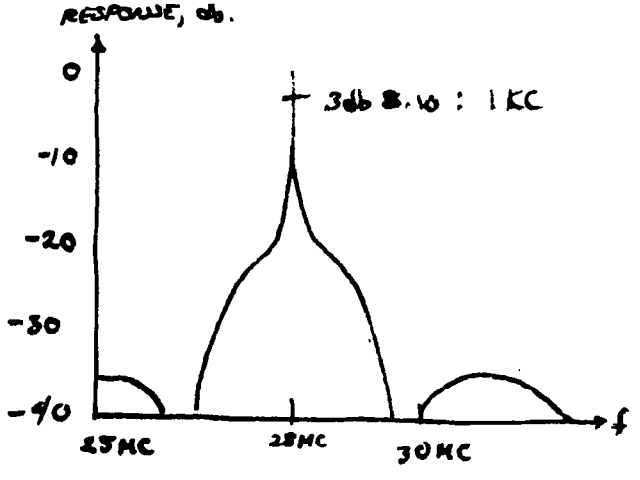

FIGURE 26

FILTER & AMPLIFIER FREQ. RESP.

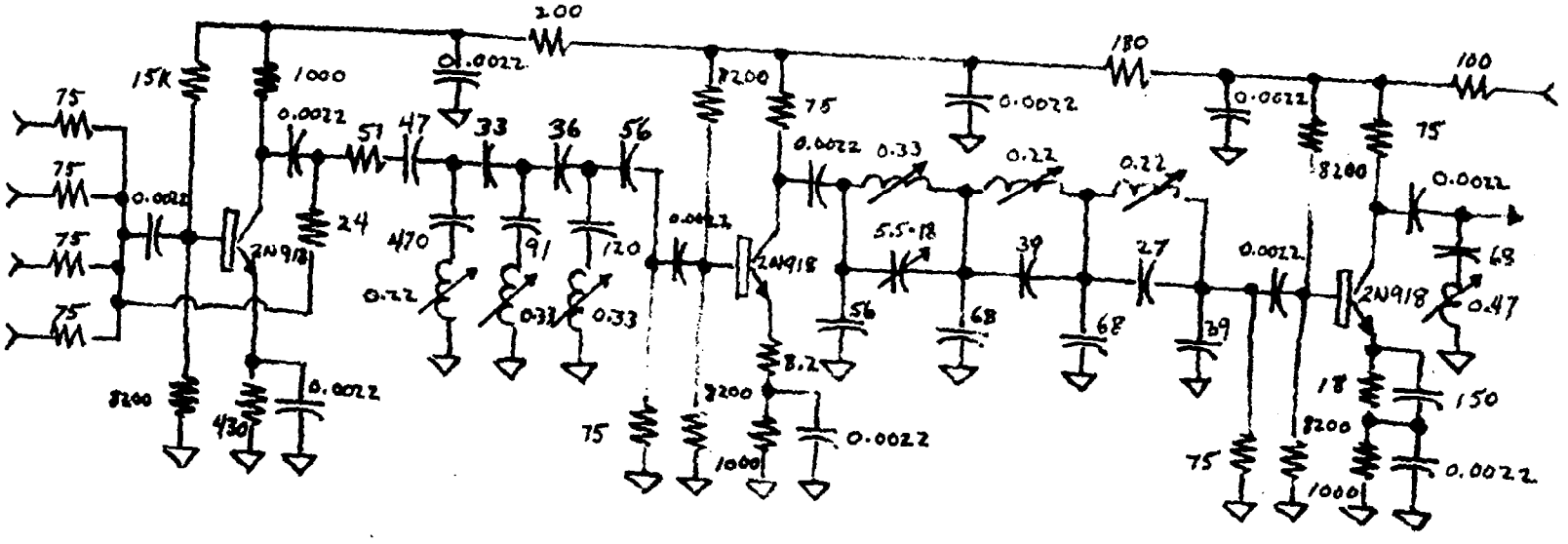

FIGURE 27 COMBINER & F. TER SCHEMATIC

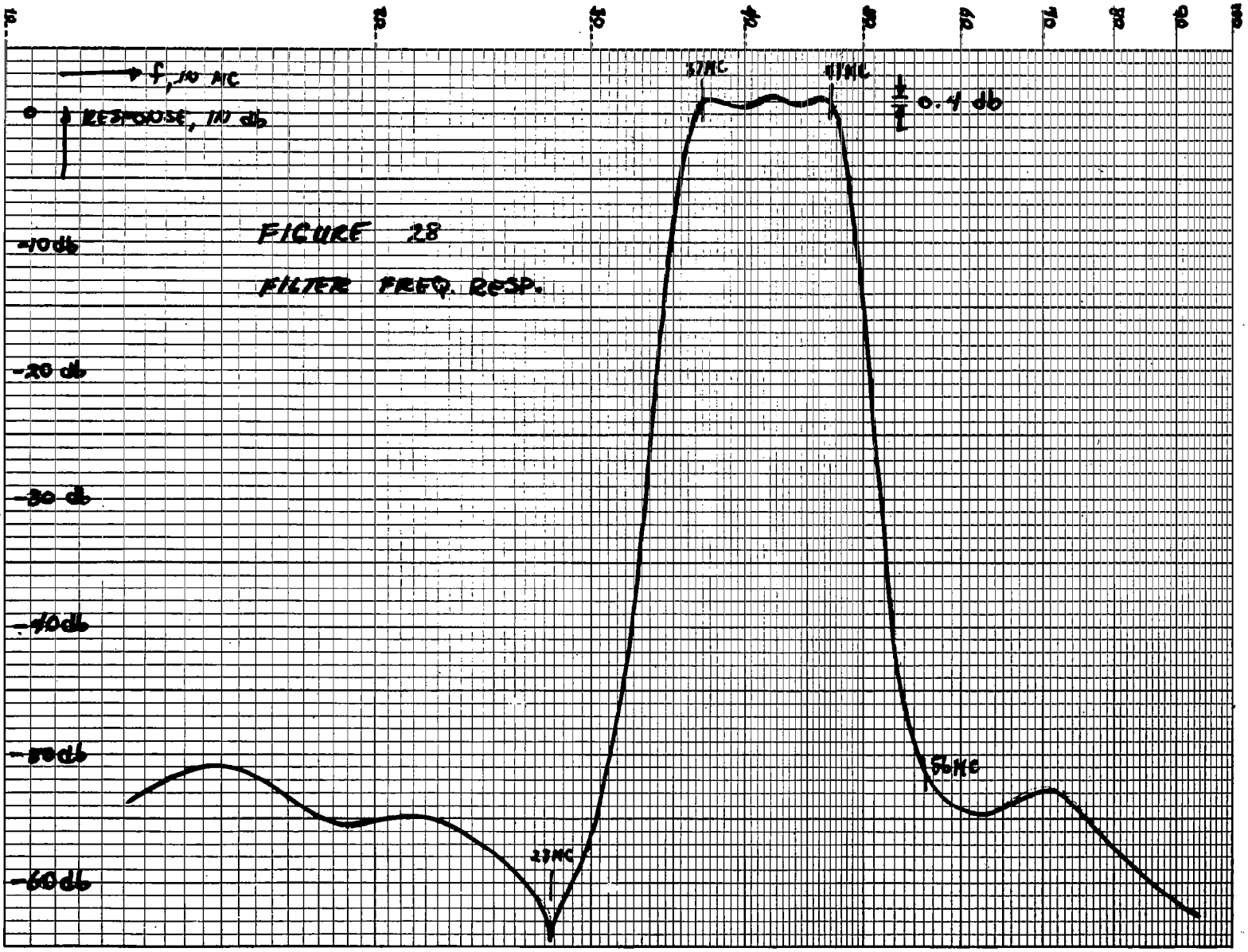

FIGURE 28

FILTER FREQ. RESP.

The output amplifier is to have a gain of 21 db and to be flat 37 - 47 MHz. It must also have the capability of driving five 75 ohm loads (four modulators and the output) to permit the amplifier to be used for an n=4 system.

The unit was designed to be a self-contained AGC amplifier so that the SPI loop could be closed without AGC applied to the system inputs. Under normal conditions, the AGC circuits in the amplifier are connected to a fixed bias to provide the 21 db of gain required.

The amplifying stages are common-emitter stages arranged two in pairs with the AGC attenuators before each pair. An emitter-follower is used as a low impedance output stage to drive the 75 ohm outputs.

The attenuator stages are made up of four silicon high speed diodes arranged in a π-pad configuration. The AGC voltage varies the current through different arms to provide varying attenuation. The frequency response is quite flat (0.5 db over 20 db attenuation range) and the attenuation can be as high as 30 db. Minimum loss is 3 db.

The AGC detector is made up of a signal amplifier, a peak-to-peak detector, and a DC amplifier. The AGC loop gain is thus very high. The AGC time constant is fixed by the R-C at the input to the DC amplifier divided by the loop gain. This is 25 msec for this design. The gain of the signal amplifier and the reference for the DC amplifier are chosen to fix the system output level to -20 dbm.

The schematic is given on Figure 29, and output level versus input level is shown on Figure 30.

This completes the description of the basic SPI blocks. The blocks contained in the input signal preconditioner unit are needed only to provide the AGC, noise addition, and delay-cancelling functions.

The noise filter is a simple 70 MHz bandpass type that can be adjusted for bandwidths from three to ten MHz. Its output is added to the signal input with enough isolation to prevent the return loss of the filter from affecting the input circuit.

The AGC circuit is the same type used in the output amplifier. The AGC control line, however, is isolated with an emitter follower DC amplifier stage. This permits the AGC to drive many such units to permit operation of an n=4 system.

The attenuator is followed by a single stage 70 MHz amplifier to provide 12 db of gain to recover the losses in the attenuator.

The delay cancellation must be made up of two parts. The delay that the signal experiences in the second modulator, 37 - 47 MHz filter, and the output amplifier is made up of a constant pure delay (in the amplifier stages) and a component that is a strong function of frequency, because of the action of the 37 - 47 MHz bandpass filter. The delay in the amplifier stages was measured and found to be 14 nsec. This was cancelled by a 10 ft. piece of subminax cable. The delay of the filter was cancelled by building another filter with the same frequency response but

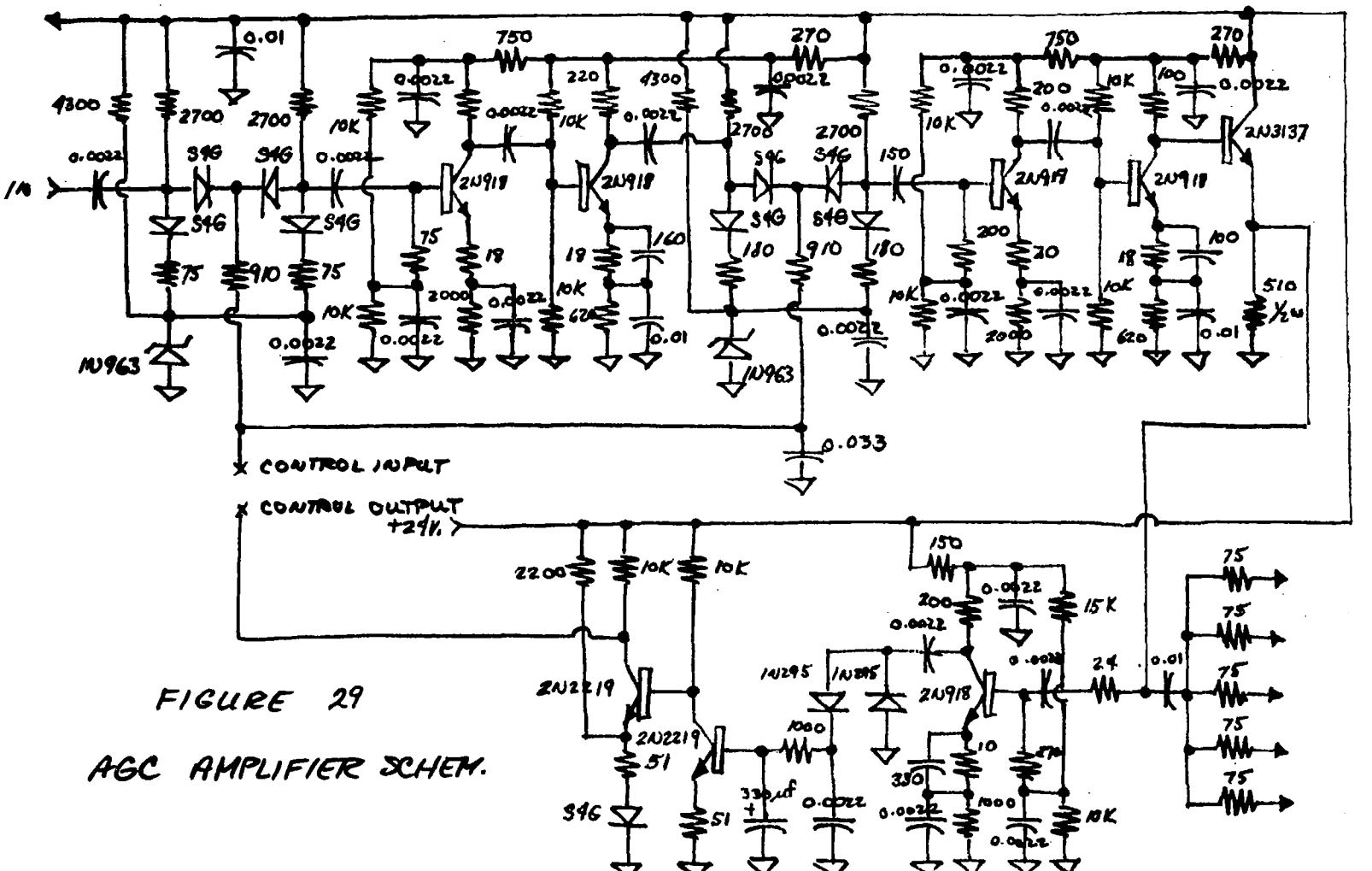

FIGURE 29

AGC AMPLIFIER SCHEM.

FIGURE 30

AGC AMPLIFIER GAIN REGULATION

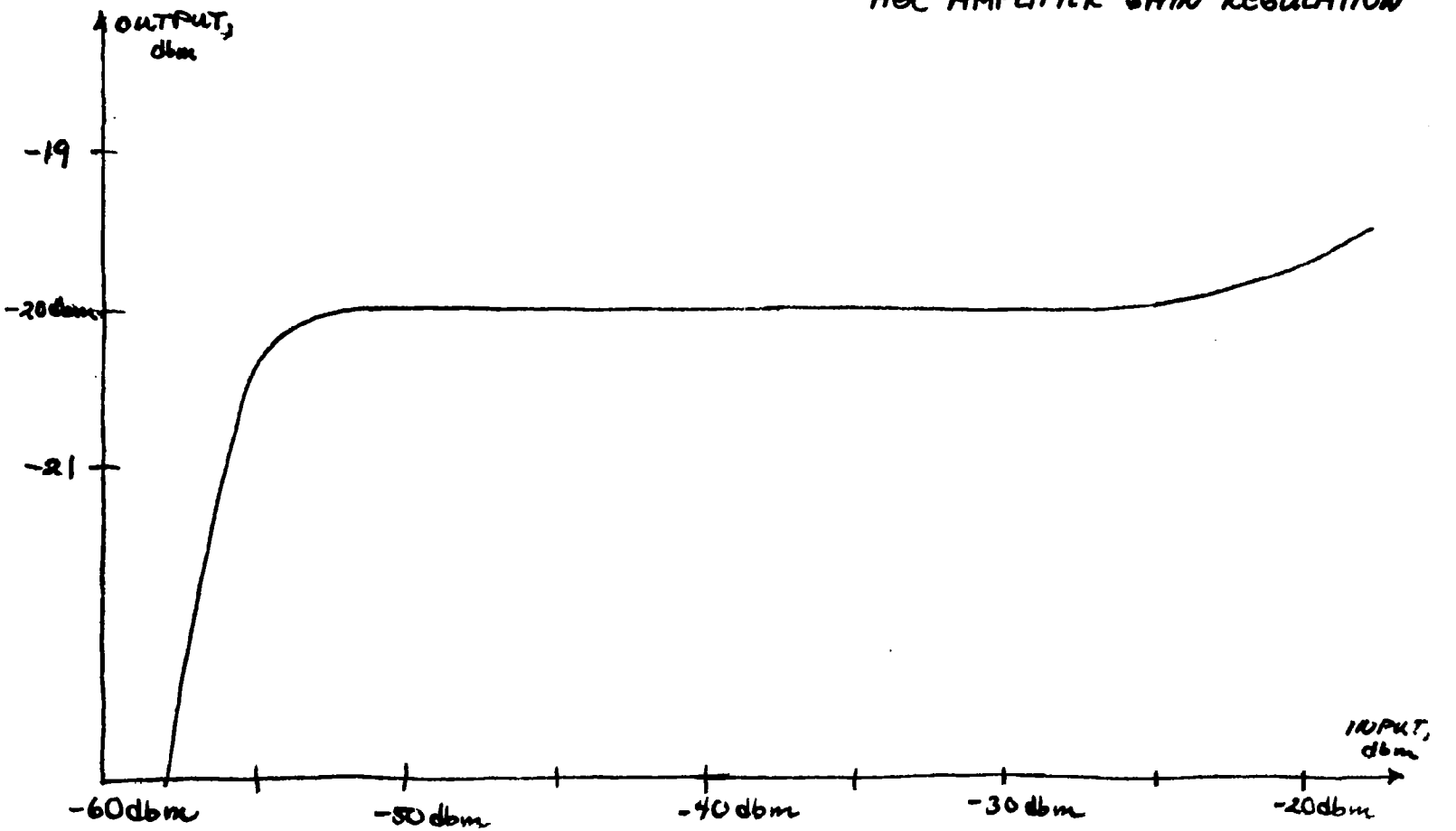

shifted to the 67 - 75 MHz band. It was assumed that two filters with identical low pass transformers would have identical delays. This filter was an elliptical bandpass design, and because of the high order structure of the 37 - 47 MHz filter, was quite complicated.

The schematic of the entire signal preconditioner unit is shown on Figure 31, and the frequency response from the signal input to the output of the delay cancellation filter is shown on Figure 32. Of note is the high degree of similarity to the response of the 37 - 47 MHz filter shown on Figure 28.

Printed circuit panels with the various functions for the SPI processor block were mounted in 15-inch shielded cans with appropriate connectors. The layout is shown on Figure 33. Two such channels were then aligned to be as identical as possible in characteristics.

The panels for the signal preconditioner blocks were assembled in nine-inch cans. The layout is shown on Figure 34. Two of these were tuned to be as close as possible. In addition, by trimming resistor values the two AGC circuits were made to track within 0.5 db over a 10 db range.

The panels for the combiner, filter, amplifier, and AGC detector were mounted in a 15-inch can as shown on Figure 35. The filter was aligned to be as flat as possible over 37 - 47 MHz while rejecting 28 and 56 MHz.

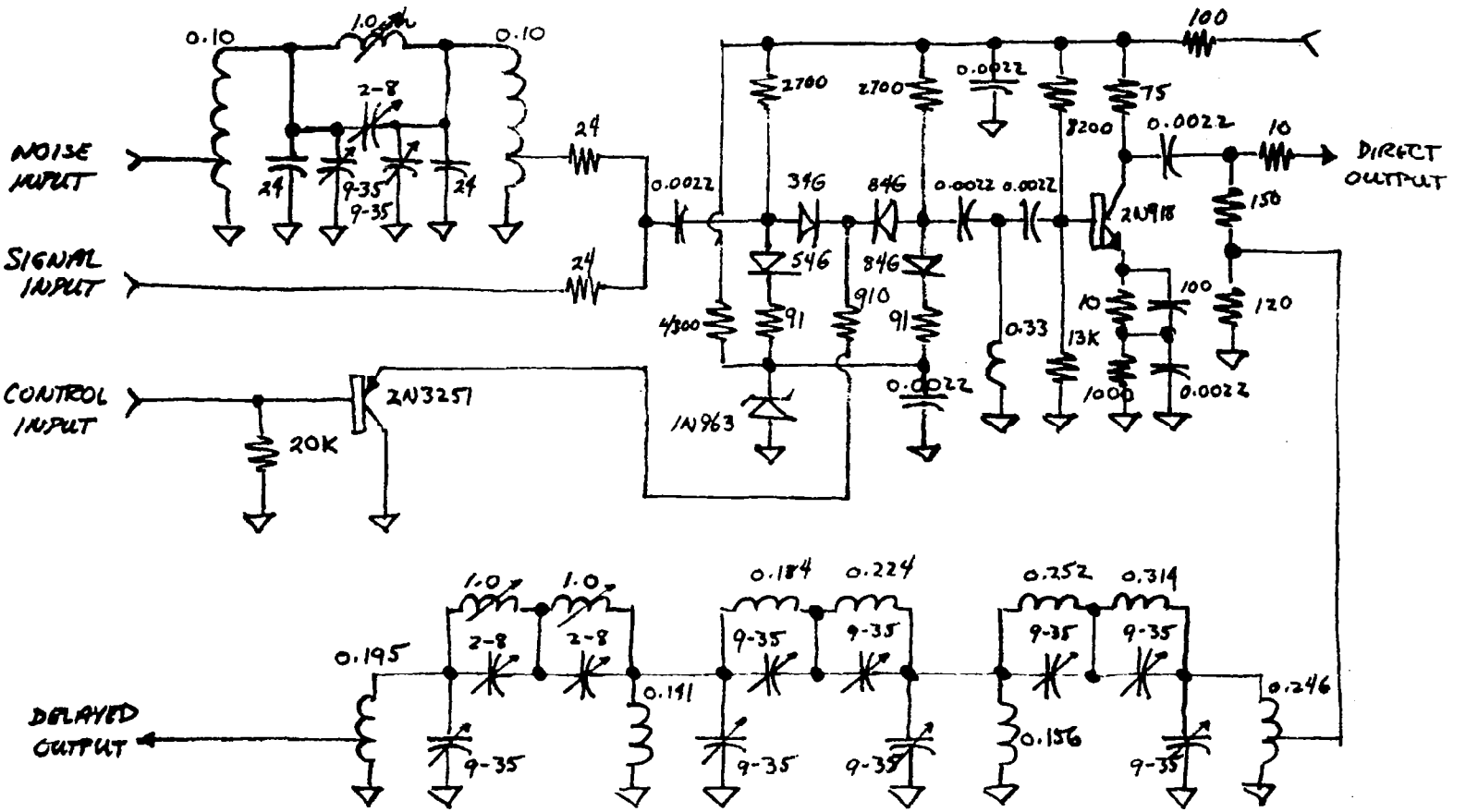

FIGURE 31

SIGNAL PRECONDITIONER SCHEMATIC

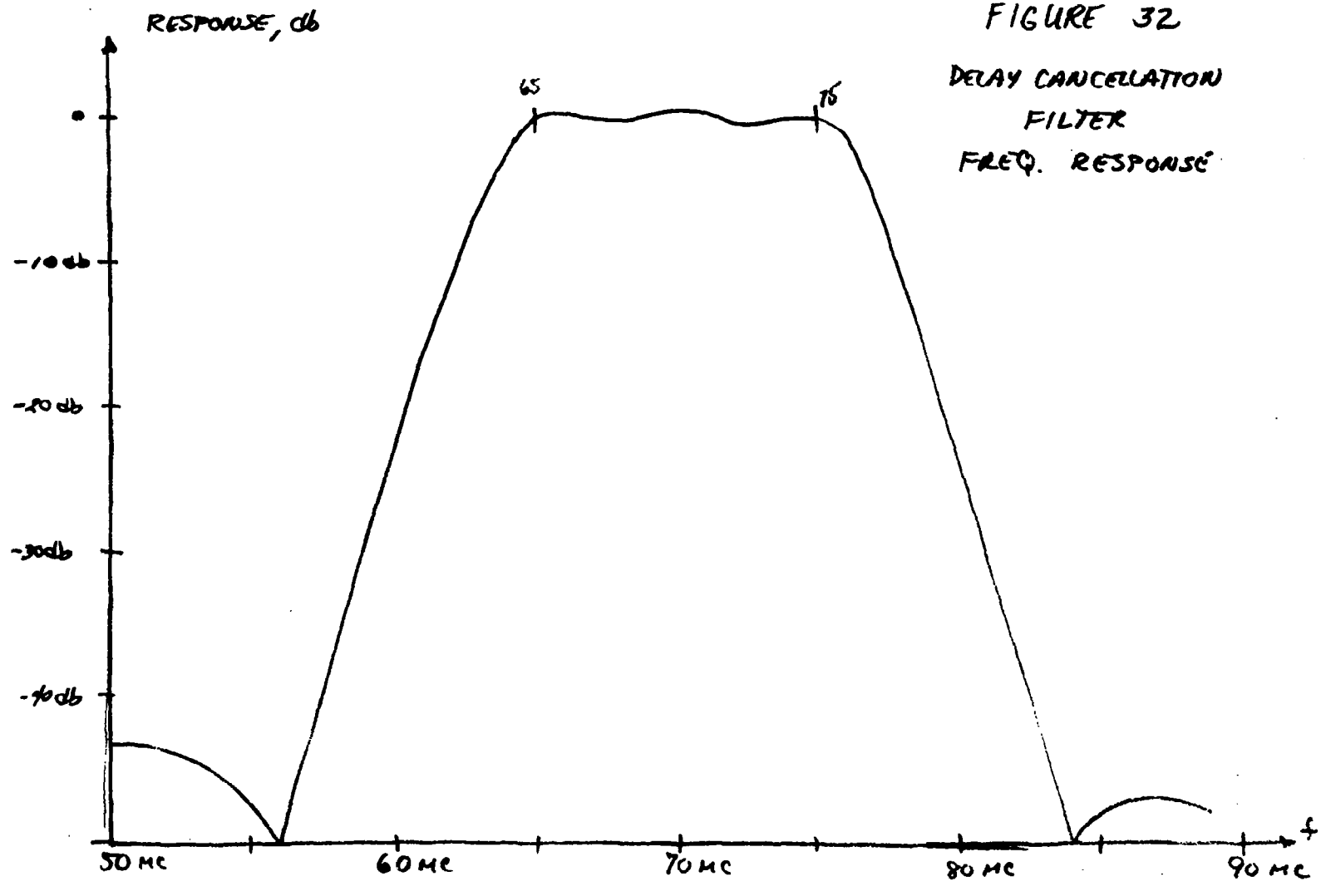

FIGURE 32

DELAY CANCELLATION FILTER FREQ. RESPONSE

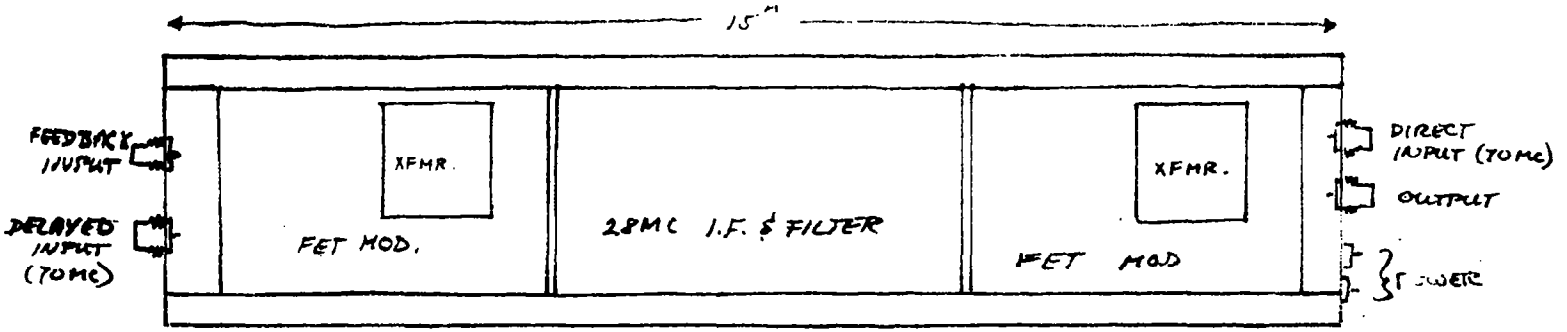

FIGURE 33 PROCESSOR LAYOUT

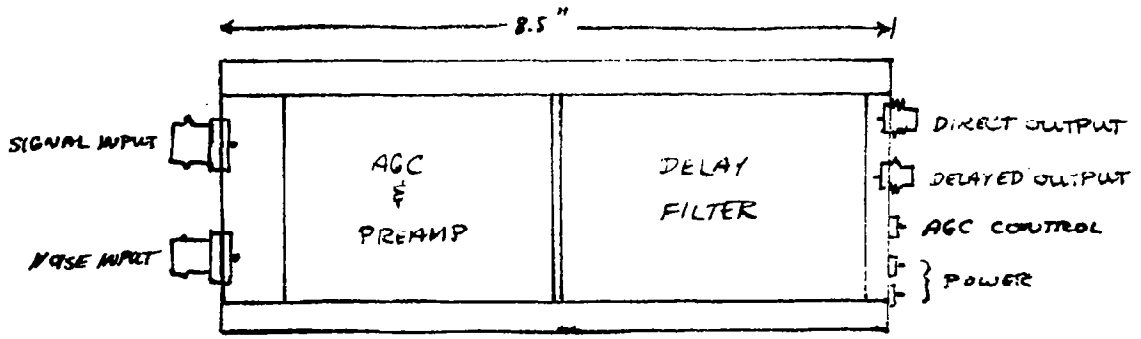

FIGURE 34 SIGNAL PRECOND. LAYOUT

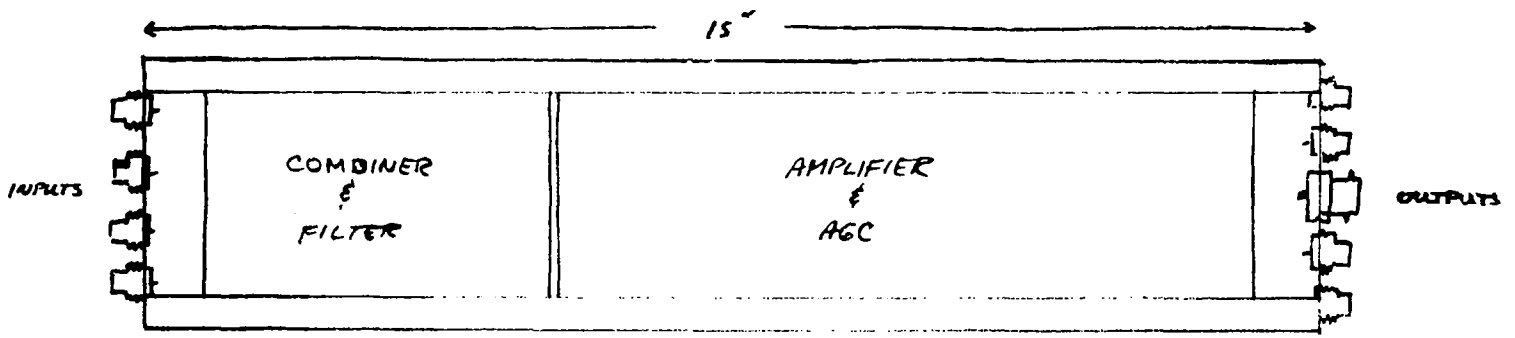

FIGURE 35 COMBINER, FILTER, AMP LAYOUT

One signal preconditioner and one SPI processor were connected with the combiner can to form a one-channel system. This was connected as shown on Figure 36. A 70 MHz signal (-6 dbm) was connected at the input and the IF tuning was adjusted to give maximum AGC voltage. The point of maximum AGC voltage should occur when the phases are all correct around the loop.

The 70 MHz signal was changed to a 65 - 75 MHz sweep. The sweep rate was made as high as possible to prevent the AGC time constant from allowing the AGC to follow frequency response deviations. A logarithmic amplifier, oscilloscope, and marker generator were set up to observe the response as shown on Figure 37. The trimmer capacitors on the FET modulators were then adjusted to give widest, flattest frequency response, and the delay cancellation filter was touched up to further help the response. (It should be noted that although the sweep was too fast for the AGC to follow, it was too slow to prevent the amplitude of the IF from following fluctuations in correllation. Therefore, this is a sensitive method for matching the delays.) The IF tuning was then touched up to remaximize the AGC voltage.

The second set of units was then placed in the system and the first set removed. The same alignment procedure was followed, with special attention given to getting an identical response and an identical AGC voltage.

The two channel SPI combiner was connected as shown on Figure 38. The loop of cable and the coaxial switch allow a phase shift of about 160° to be placed in one input leg to test the SPI action.

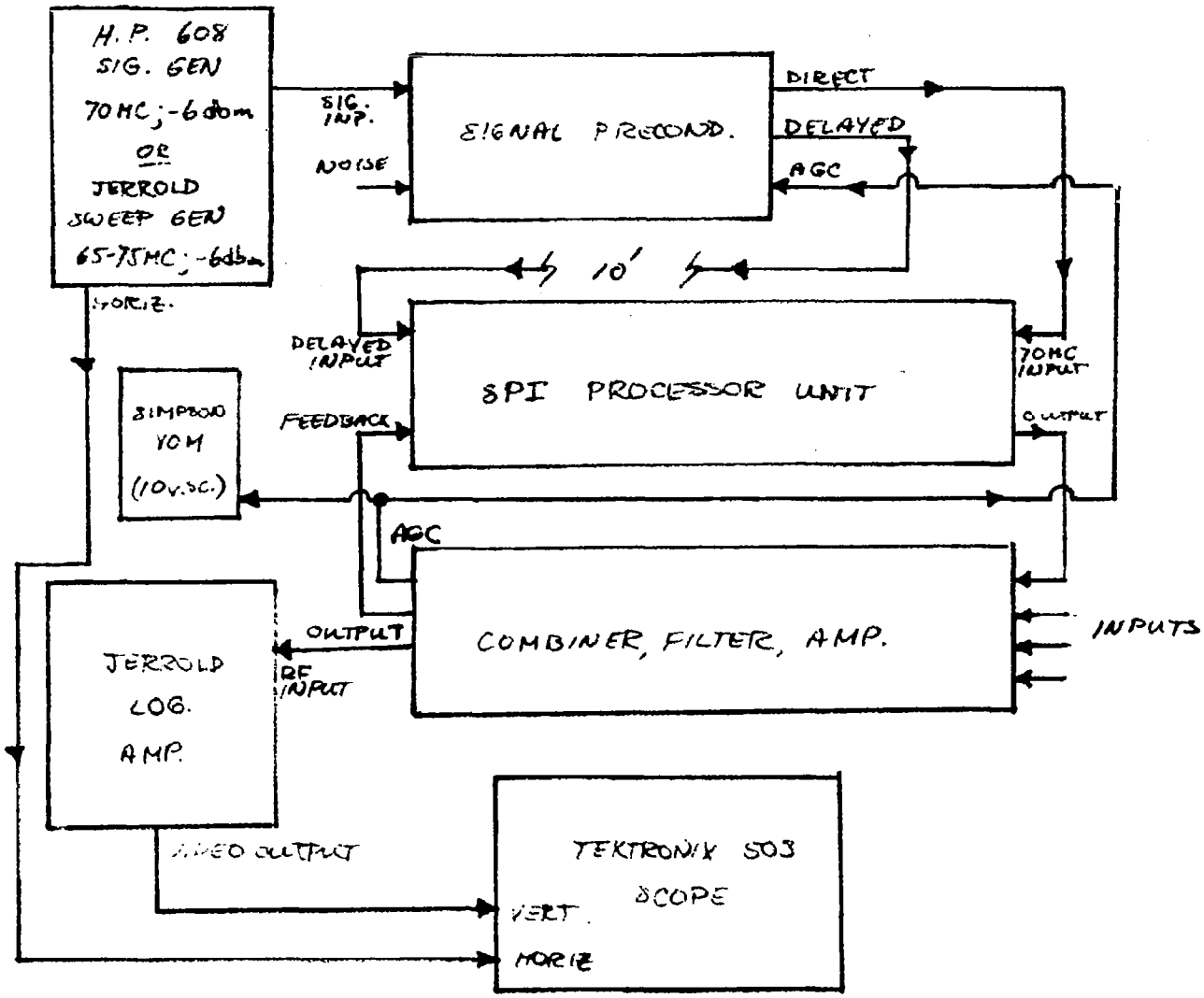

FIGURE 36 SINGLE CHANNEL TEST SET-UP

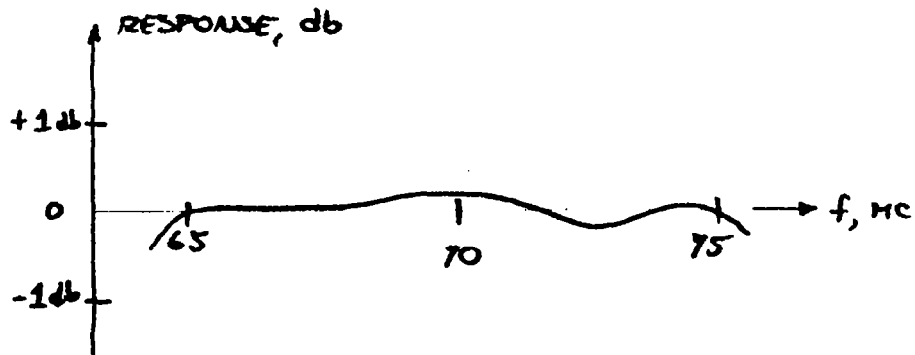

FIGURE 37 SINGLE CHANNEL FREQ. RESP.

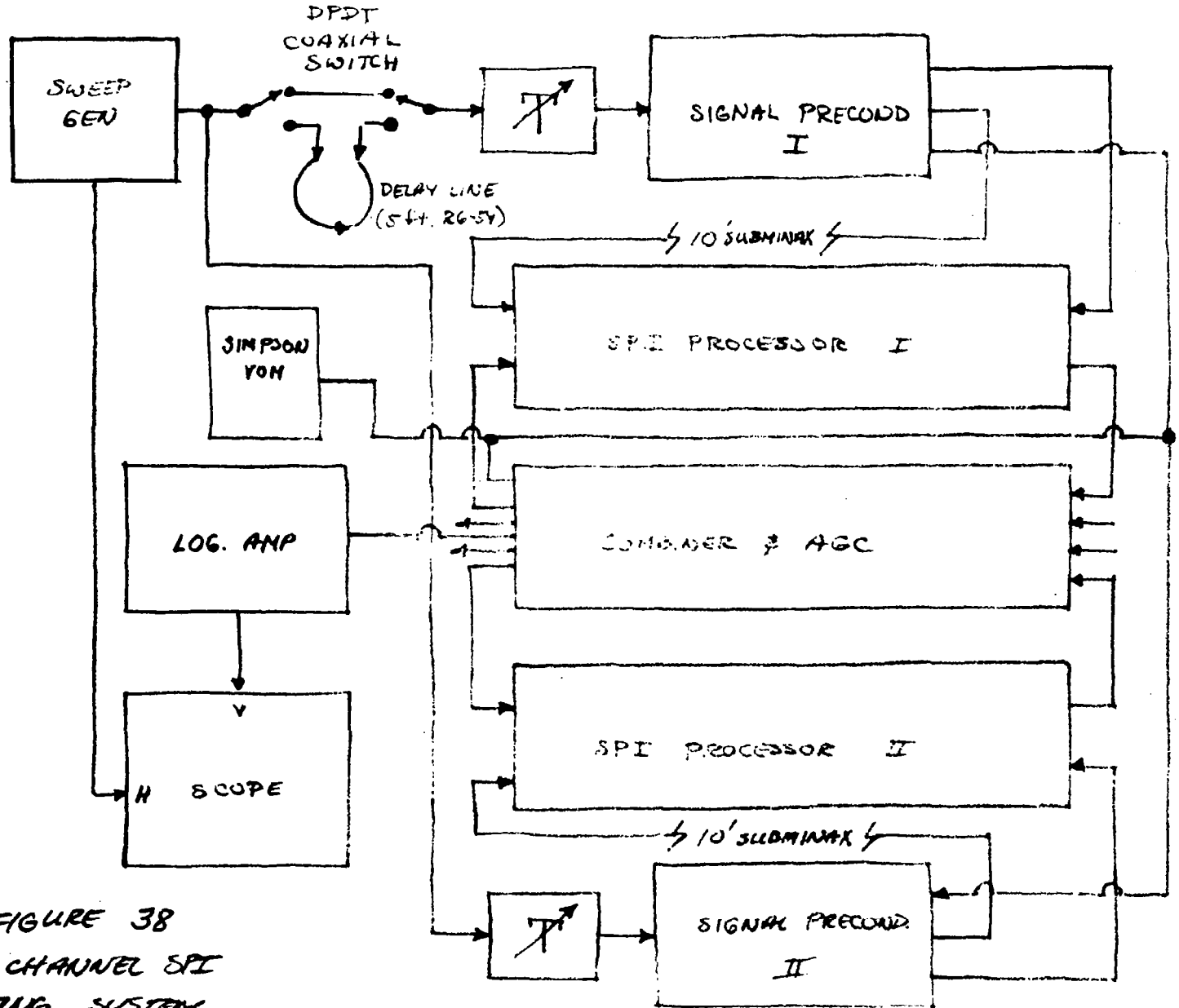

FIGURE 38
TWO CHANNEL SPI
TESTING SYSTEM

The input to one channel was disconnected and the response of the other channel checked. Some touching up of the adjustments was necessary because of the loading effect of the second channel. The IF of the off channel was observed by sampling scope to be (because of modulator imbalance, leakage, and radiation) only about 20 db below that in the on channel. This is not ideal performance, but does not make a significant difference in the system test results.

The second channel was then turned on, the first turned off, and the above repeated.

Both channels were turned on, and the IF tuning of both adjusted for maximum AGC voltage. A maximum indicates that in-phase voltage addition of the inputs is taking place. The coaxial switch was flipped to place 160° of phase shift in one channel, and it was observed that the AGC was still at a maximum. A dual trace sampling scope was connected to the two 28 MHz IF signals, and it was observed that when one input phase changed, the phase of that IF changed by the same amount, showing proper SPI action. In addition, in phase operation was indicated by noticing that the AGC attenuation changed by 3 db when one input was removed. Because of the signal-squaring behavior of the processor, this indicates 6 db addition at the combiner.

Figure 39 shows the frequency response of each of the two channels and the sum. Notice the small change when the phase of one is changed. This is caused by the small 28 MHz leakage from one IF to the other, thus changing the channel characteristics slightly when the phase is changed.

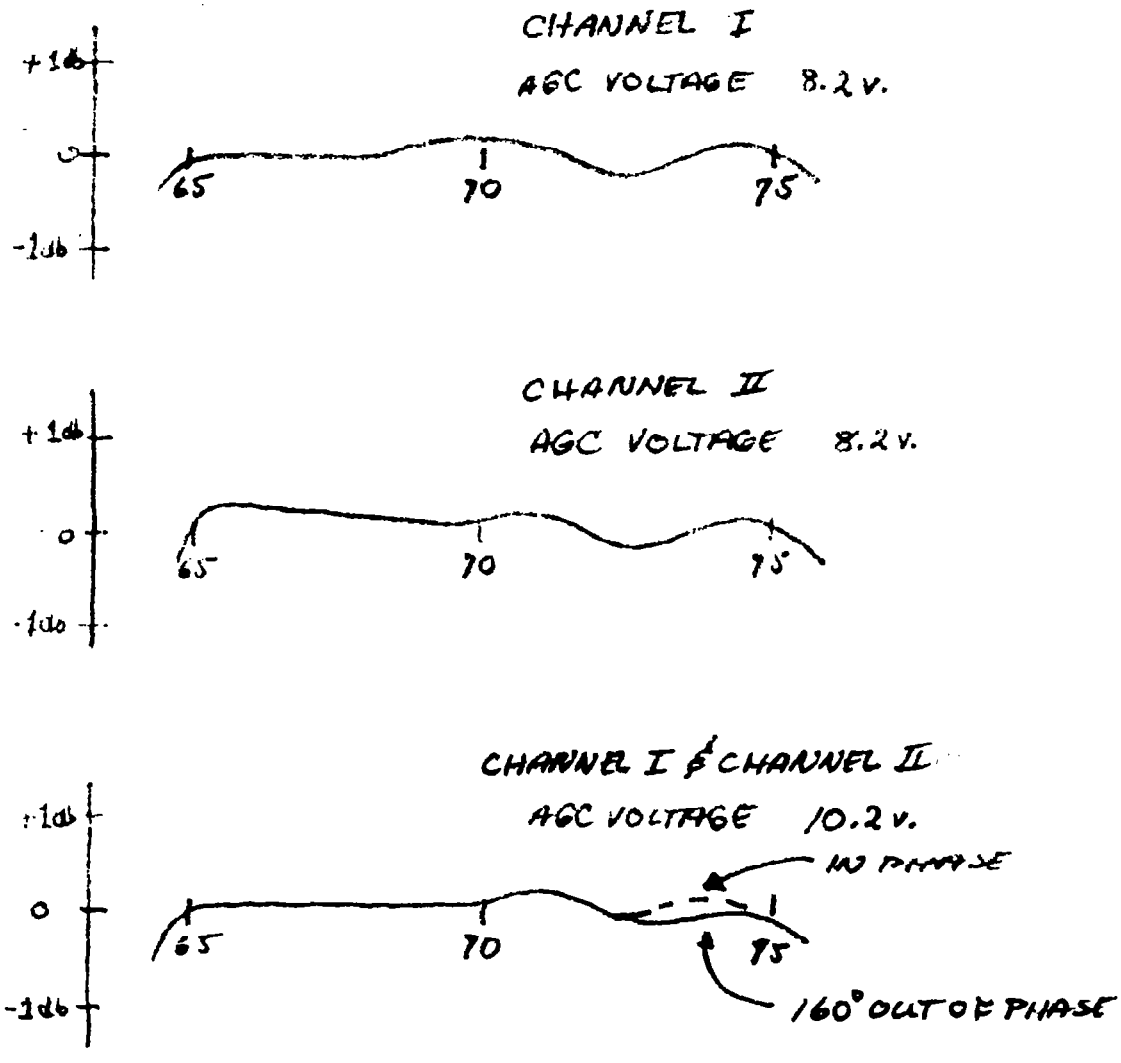

FIGURE 39

TWO CHANNEL SPI FREQ. RESP.

Figure 40 shows the AGC voltage plotted against input level for each channel. A third curve is plotted for both channels together. Note the 3 db shift, indicating voltage addition.

In order to test the SPI combiner for ratio-squared combining, a set-up was devised that would effectively measure the weighting of the two input channels. Figure 41 shows the set-up.

Reference input was taken to be -6 dbm at the signal inputs and +1 dbm at the noise inputs (the difference is because of the 7 db pad in the signal preconditioner unit to isolate the filter).

The first test made was to verify the theoretical prediction that if uncorrelated signals were applied to the inputs the only output would be due to the stronger. Oscillator 1 was tuned to 68 MHz and +1 dbm, and oscillator 3 was tuned to 72 MHz and the output varied from +1 dbm down to -5 dbm. The ratio of the levels at the selective voltmeter (40, 44 MHz) was plotted against the ratio of the input levels. Oscillator 3 was then fixed at +1 dbm and oscillator 1 varied to plot the other half of the curve. Figure 42 shows the results.

It should be noticed that over a 30 db range in output rejection ratio the line is nearly a perfect match to the theory. The reason that the curve breaks away from the ideal is that there is, as mentioned before, a small leakage of 28 MHz IF signal from

FIGURE 40

AGC VOLTAGE

VS

INPUT LEVEL

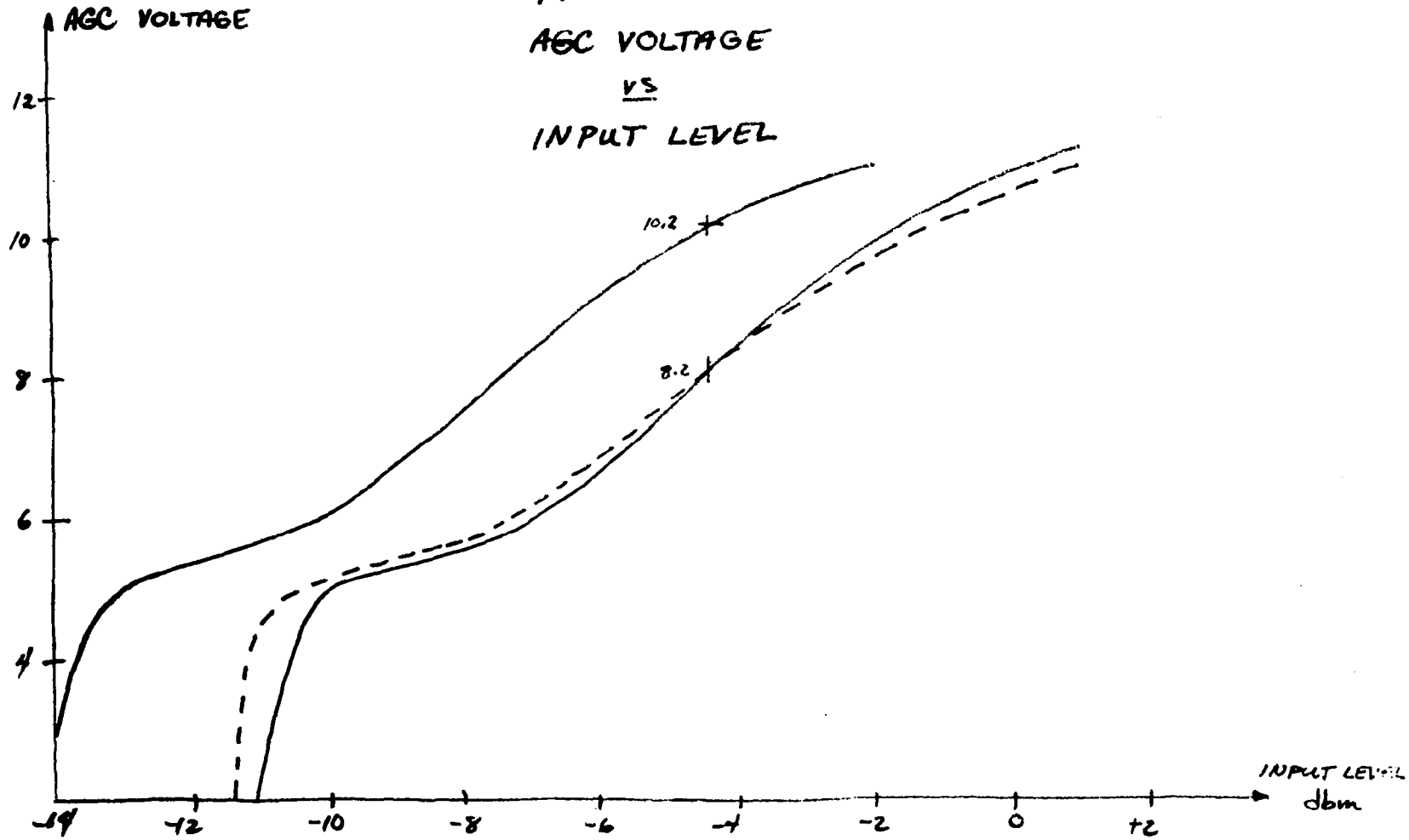

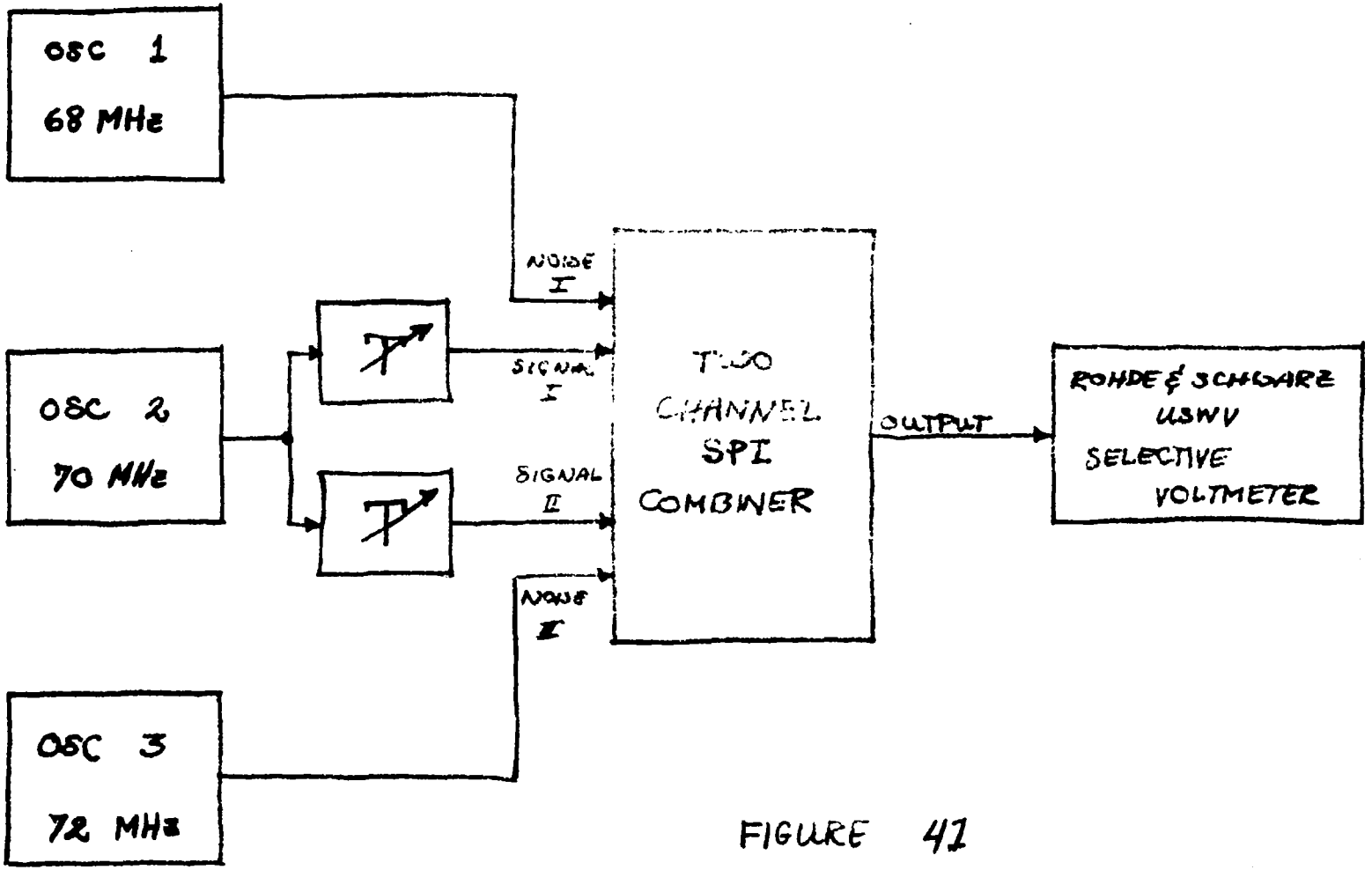

FIGURE 41

RATIO SQUARED COMBINING

TEST SET-UP

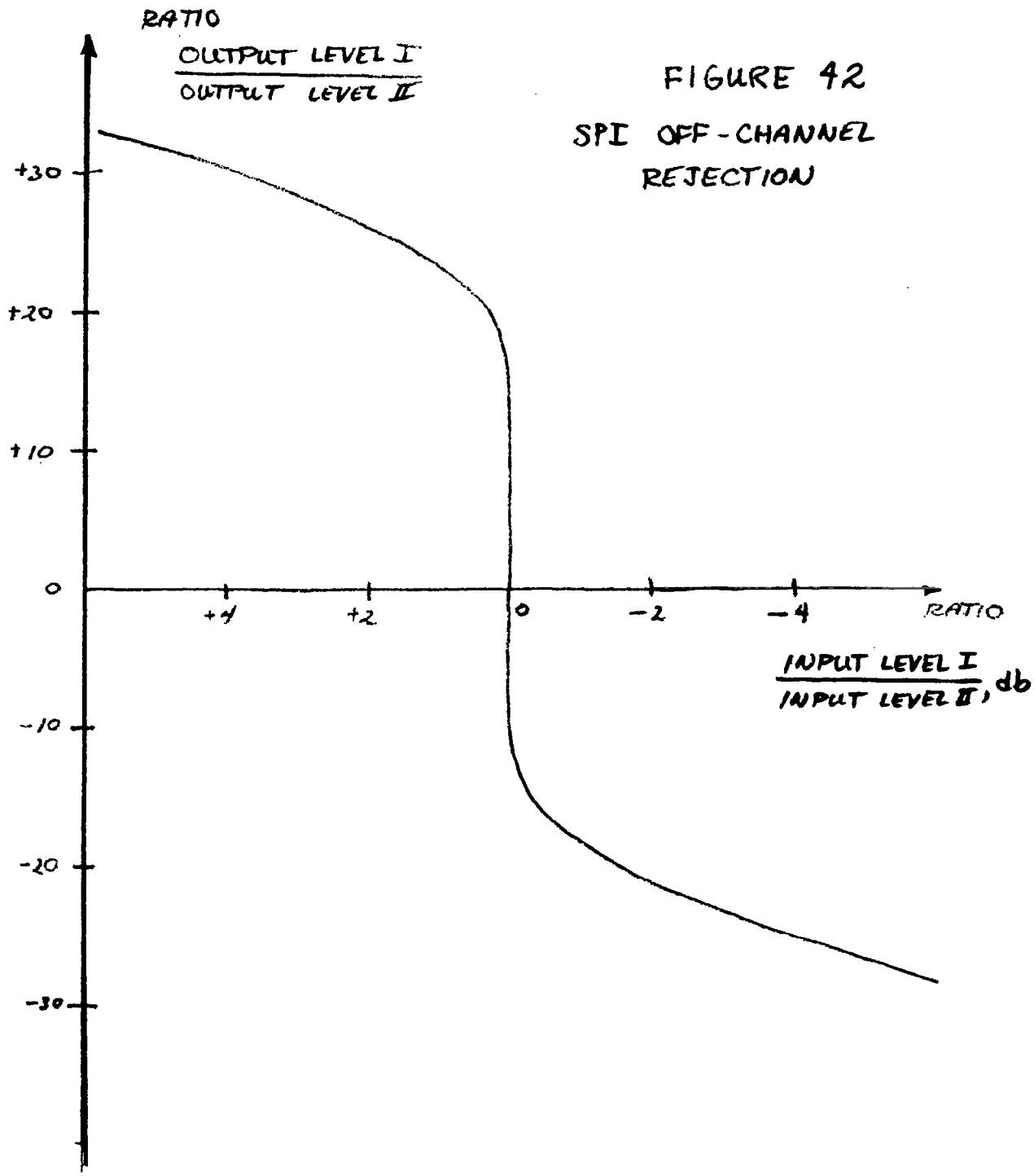

FIGURE 42

SPI OFF-CHANNEL REJECTION

one channel to the other. This leakage is down about 20 db, and that is approximately the point at which the curve departs from theory.

This indicates that ratio-squared operation can be expected over a 20 db spread in input signal strengths without having to improve off-channel rejection. This should be adequate for almost all applications.

Both oscillator 1 and oscillator 3 were then set at -9 dbm, and oscillator 2 was set to 70 MHz and +4 dbm. 10 db was placed in each pad. The system output gave a 42 MHz signal at -20 dbm and 40 MHz and 44 MHz signals at -36 dbm, indicating that the 70 MHz inputs were adding in phase. The 40 MHz and 44 MHz tones, being incoherent, add in power, and so the "signal" (42 MHz) to "interference" (40 and 44 MHz) ratio was improved by 3 db. One of the attenuators was used to lower the signal in that path, and the signal to interference ratio was computed and plotted on Figure 43. The same process was repeated for the other channel, but no difference was detectable. The resulting curve precisely follows the theory.

The two attenuators were returned to 10 db, and the "interference" oscillators 1 and 3 were increased to +1 dbm. The "signal", oscillator 2, was then decreased. The equal-input combining improvement was measured and found to hold to 3 db even when the "signal" was 20 db below the "interference" as plotted on Figure 44. This indicates that a similar situation will apply to noise inputs since the bandwidth of the IF filters is very small.

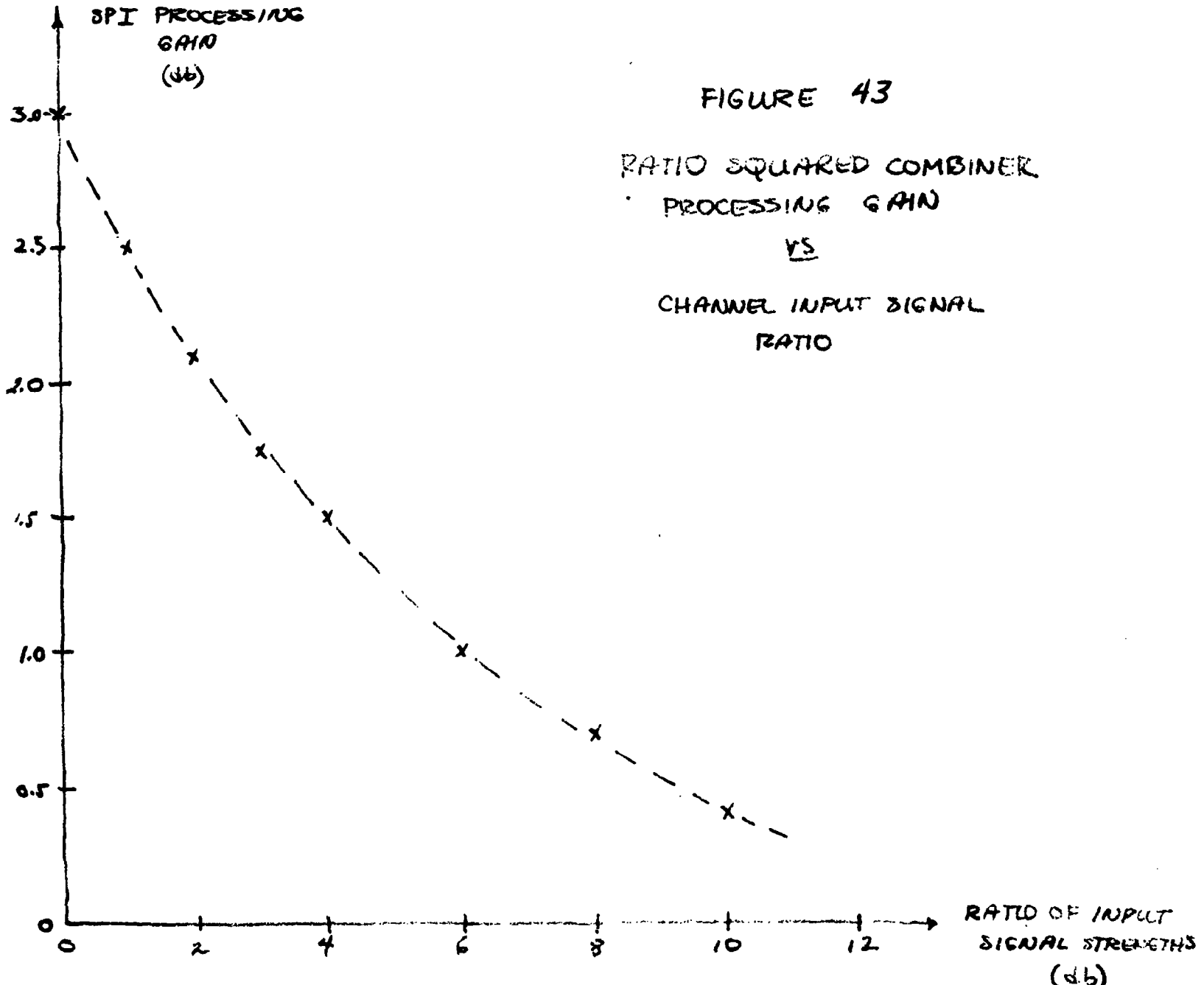

FIGURE 43

RATIO SQUARED COMBINER PROCESSING GAIN

VS

CHANNEL INPUT SIGNAL RATIO

FIGURE 44

PROCESSING GAIN
VS
SIGNAL / INTERFERENCE
RATIO

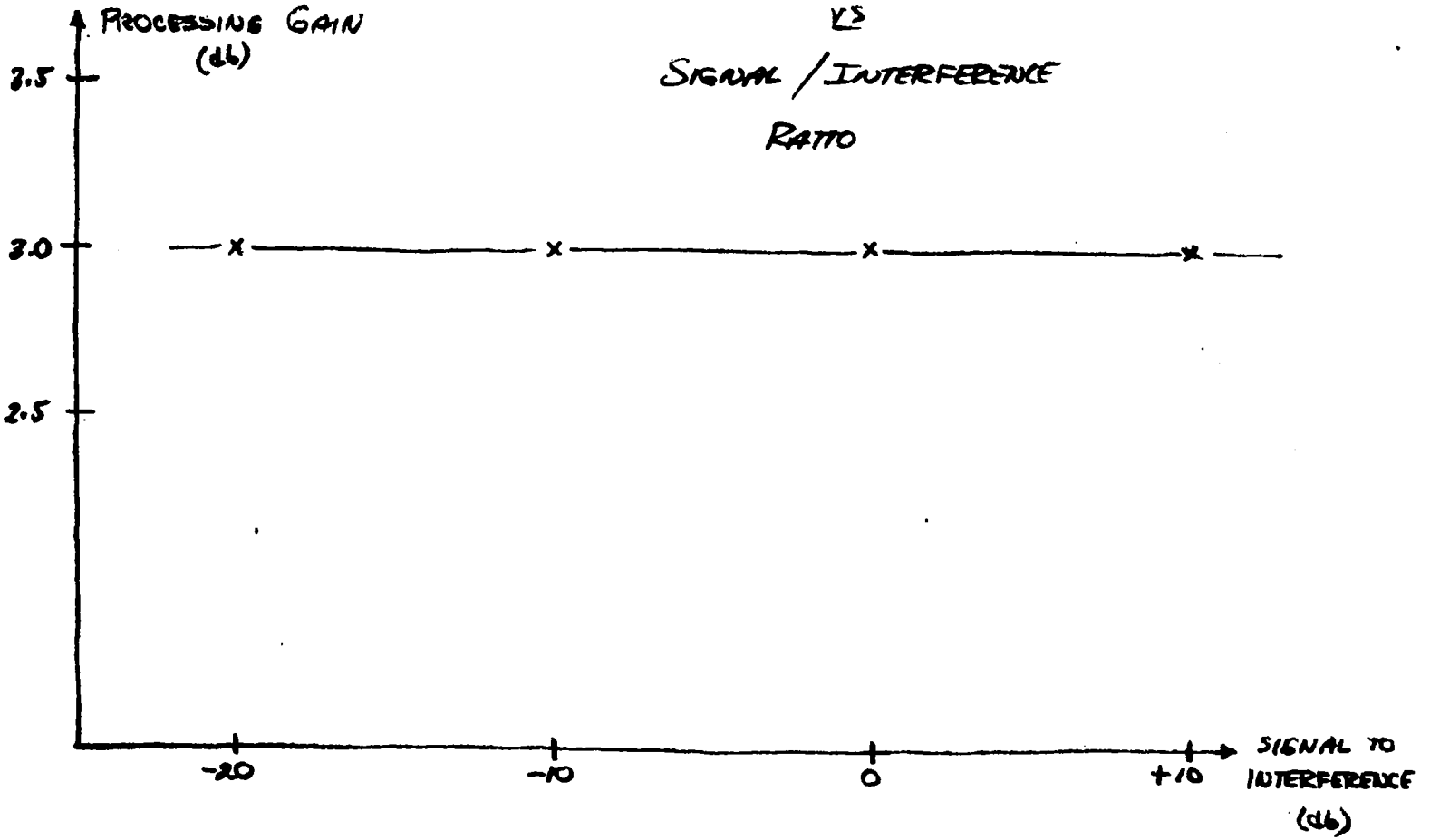

Intermodulation distortion was measured with the set-up of Figure 45. The two oscillators were set at 69 MHz and 71 MHz, and outputs then resulted at 41 and 43 MHz. Distortion products were then measured at 39 MHz and 45 MHz as a function of input level and plotted on Figure 46.

The source of this distortion appears to be the AGC diode attenuators, since they are the only non-linear elements in which the level changes as the input is varied. A way to reduce this problem is to change the type of AGC to a more linear system with F.E.T.'s or perhaps Raysistors.

The experimental SPI combiner thus proved the theory correct. The phase of the signal at the input was shown to have no effect on the output phase, and ratio-squared combining was demonstrated. A frequency response of 10 MHz was achieved, thus indicating the feasibility of using the SPI principle for combining wideband signals at IF.

Many improvements could be made in the electrical design. This was a breadboard evaluation whose purpose was to prove the SPI concept at high frequencies and bandwidths, and not to design optimal circuits.

Electrical redesign of some sections could improve performance considerably in the frequency response and distortion areas. The system could be made to work for much lower input levels, and IF rejection in an off channel could be improved.

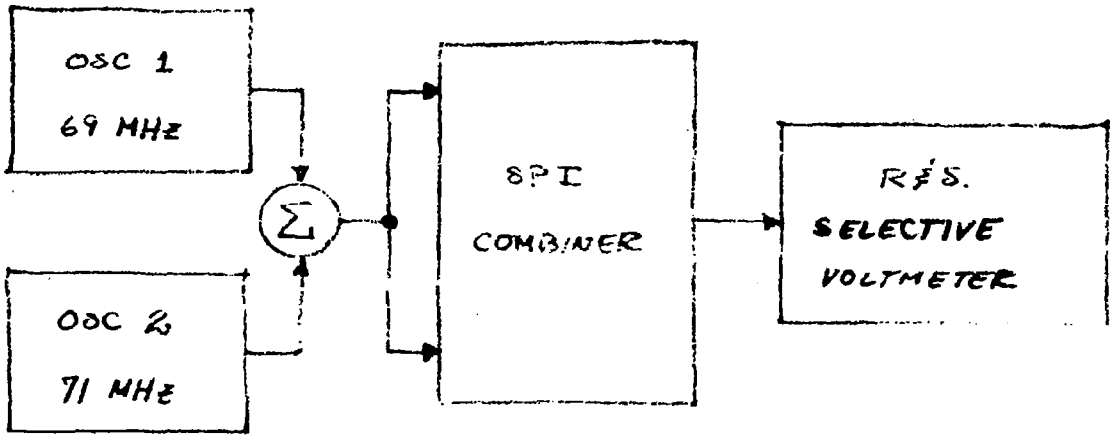

FIGURE 45

MEASUREMENT SET-UP FOR INTERMODULATION

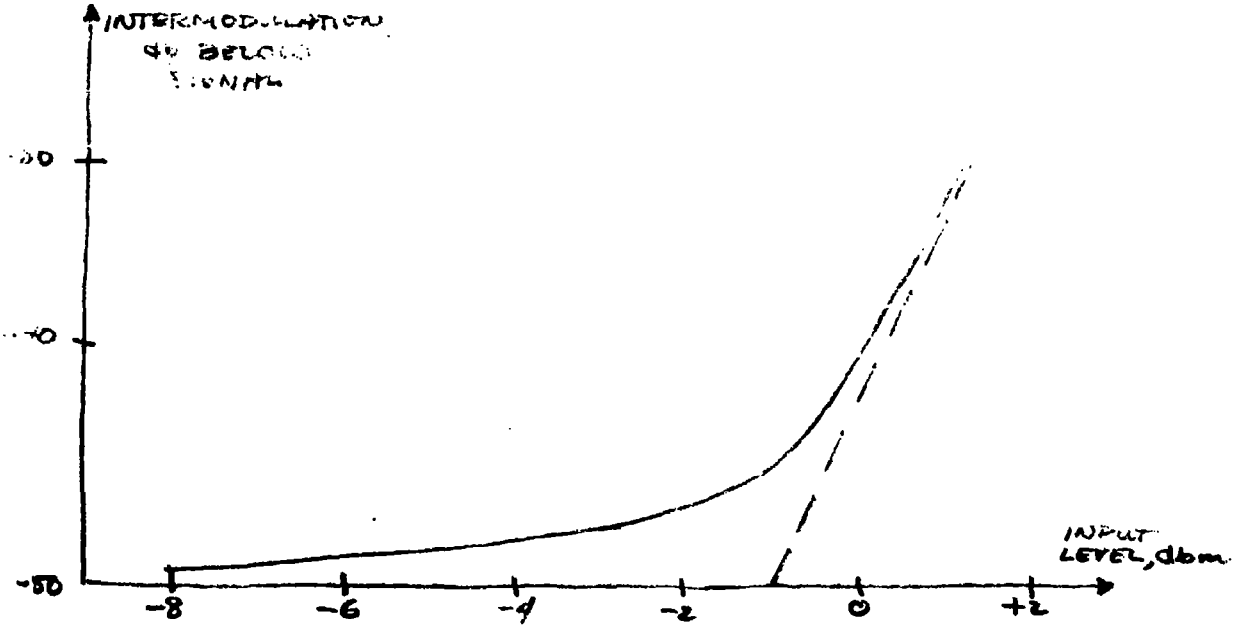

FIGURE 46

INTERMODULATION VS INPUT LEVEL

There are several additional tests that should be made to evaluate the SPI concept for predetection combining. The noise perturbation theory was not investigated, and to do so would require redesign to widen the IF bandwidth so that the amplitude fluctuation noise could be seen (for the n=2 system constructed, the amplitude fluctuation voltage amounts to about 3% of the output noise). The same would be true of the rms noise deviation measurement to evaluate phase noise. These measurements would have to be carried out at low S/N ratios, and thus two high level independent sources of 10 MHz wide noise at 70 MHz are required. These would have to be the result of a development or purchasing program, as they are not available at present.

A second characteristic that should be evaluated is system performance for a large number of channels. A certain amount of electrical redesign would be necessary to alleviate the alignment problem so that more than two stages could easily be put in parallel. An evaluation for eight channels should prove the large array capability of SPI.

There is additional R and D work remaining to verify some of the predicted characteristics of the SPI processor, but the feasibility of the system has been proved and much information obtained on this novel and powerful approach to the problem of combining the information common to a number of receivers. This novel processor is shown in Figure 47. To identify the elements of signal conditioner, signal processor, and combiner one can refer to the test arrangement diagram of Figure 38.

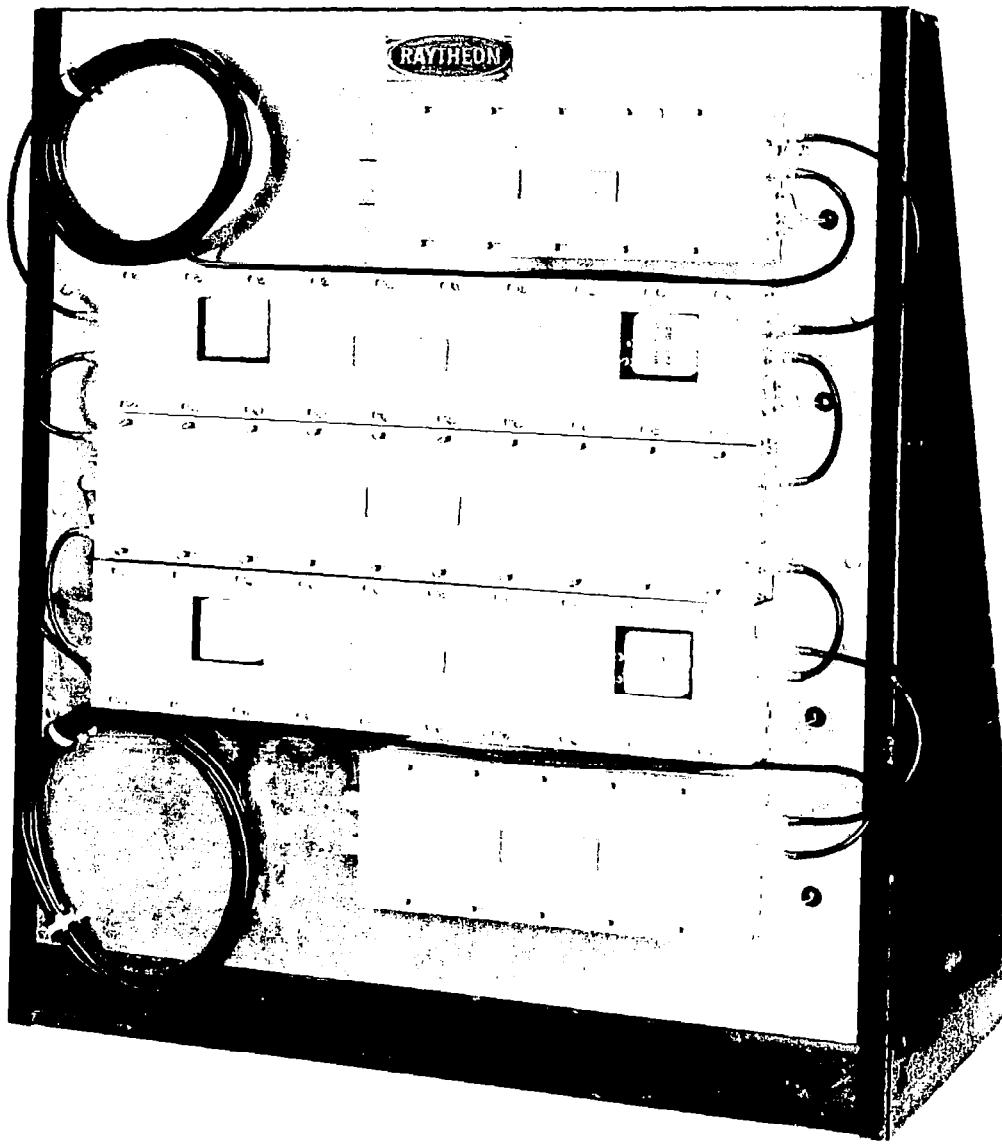

Figure 47. The Two Channel Signal Processor or Synthetic Phase Isolator

Appendix I:

LOCAL OSCILLATOR TYPE SPI

There is a second class of SPI combiners which may be useful for certain types of input signal, such as AM. The presence of a carrier is a necessity in this system, whereas the previously discussed regenerative system requires none, and works equally well with AM, SSB, PM, or any other modulation scheme.

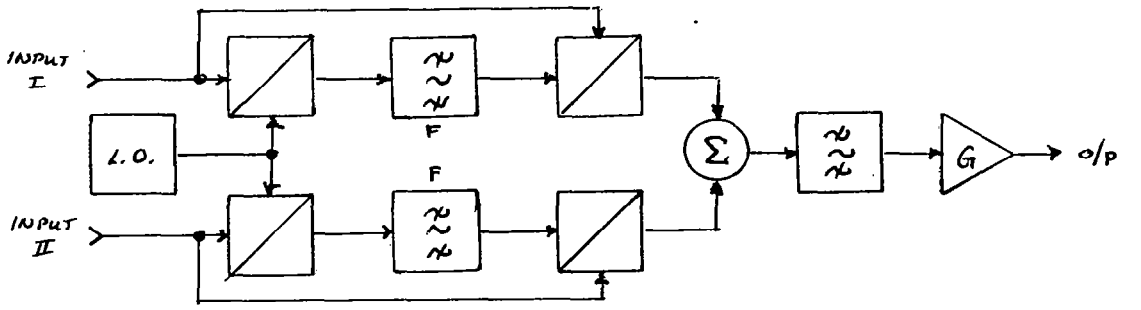

FIGURE 1

Figure 1 shows the block diagram of this type of system for n=2. If the L.O. output is $\cos(\omega_o t+\Theta)$ and the i^{th} input is given by $A_i \cos(\omega_i t+\phi_i)$, and the filter (F) is centered at $\omega_{if} = \omega_i - \omega_o$, the output will be $V_o = \frac{G}{4}\sum A_i^2 \cos(\omega_o t+\Theta)$. As can be seen, ratio-squared combining is still taking place at the summation, and the ϕ_i are removed.

If however, there is modulation on A_i, the output of the filter will not be $A_i \cos(\omega_{if} t + \phi_i - \Theta)$, but will be (for a very narrow filter) $\bar{A}_i \cos(\omega_{if} t + \phi_i - \Theta)$. Thus A_i must have a constant (DC)

component in order to give an IF level. This limits the use of this system to modulation schemes that transmit a strong carrier.

If $\phi_i = \phi_i(t)$, and no spectral components of the signal are within the passband of the filter, the IF level will be $A_i^* \cos(\omega_{if} t + \phi_i - \theta)$ where $A_i^* < A_i$ because of the power lost from the signal from exclusion of the sidebands.

The use of the L.O. system is thus limited to inputs such as AM and low index FM or PM, whereas the regenerative system has no such restriction. In addition, it is critical that the L.O. frequency be exactly $\omega_i \pm \omega_{if}$ in order for the carrier to appear in the filter. This restriction is not applicable to the regenerative case either.

If the input noise is of spectral density N_o and bandwidth W, and if the filter bandwidth is b, then the carrier-to-noise at the output of the filter is $(\bar{A}_i)^2/2N_oW$. If $b \ll W$, and if $\sum(\bar{A}_i)^2 \gg 2nN_ob$ then S/N at the combiner output is

$$(S/N)_o = \frac{[\sum \bar{A}_i \cdot A_i]^2}{2\sum(\bar{A}_i)^2 N_o W} \approx \frac{\sum A_i^2}{2N_oW}$$

This result assumes the product between IF signal and input noise at the second mixer is the only source of output noise.

If $\sum(\bar{A}_i)^2$ is not $\gg 2nN_ob$, then output noise is made up of three components: IF noise times input carrier, input noise times IF carrier, and input noise times IF noise. These combine to give the spectral density shown in Figure 2 :

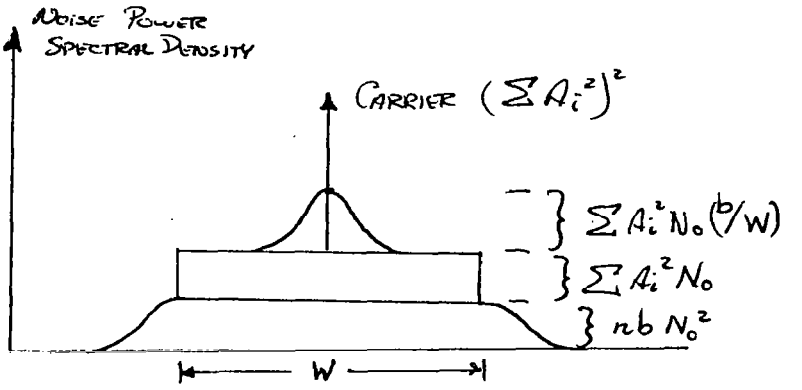

FIGURE 2

If $\sum A_i^2 \ll 2nNbb$, the output noise is essentially the noise cross product (bottom spectrum), and the output S/N is

$$(S/N)_o \approx \frac{(\sum A_i^2)^2}{nb N_o^2 W}$$

If the input frequencies are not identical, it is shown in Appendix 1A that there is an optimum value for b depending on the variation in frequency.

Experimentation and further analysis of the local oscillator SPI were not pursued because it was felt that the regenerative system is much more powerful and should receive more emphasis.

NASA-Langley, 1967 —— 7 CR-728